© 2014. Published by The Company of Biologists Ltd | Journal of Cell Science (2014) 127, 1992–2004 doi:10.1242/jcs.142083

RESEARCH ARTICLE

The polysome-associated proteins Scp160 and Bfr1 prevent P body formation under normal growth conditions

Julie Weidner, Congwei Wang, Cristina Prescianotto-Baschong, Alejandro F. Estrada and Anne Spang*

ABSTRACT

Numerous mRNAs are degraded in processing bodies (P bodies) in *Saccharomyces cerevisiae*. In logarithmically growing cells, only 0–1 P bodies per cell are detectable. However, the number and appearance of P bodies change once the cell encounters stress. Here, we show that the polysome-associated mRNA-binding protein Scp160 interacts with P body components, such as the decapping protein Dcp2 and the scaffold protein Pat1, presumably, on polysomes. Loss of either Scp160 or its interaction partner Bfr1 caused the formation of Dcp2-positive structures. These Dcp2-positive foci contained mRNA, because their formation was inhibited by the presence of cycloheximide. In addition, Scp160 was required for proper P body formation because only a subset of bona fide P body components could assemble into the Dcp2-positive foci in *Δscp160* cells. In either *Δbfr1* or *Δscp160* cells, P body formation was uncoupled from translational attenuation as the polysome profile remained unchanged. Collectively, our data suggest that Bfr1 and Scp160 prevent P body formation under normal growth conditions.

KEY WORDS: Processing bodies, mRNA, mRNA metabolism, Endoplasmic reticulum, Translation, *Saccharomyces cerevisiae*, mRNA-binding proteins, mRNA decay, Stress response, Ribonucleotide particles, Stress granules

INTRODUCTION

The protein content in a cell at any given time is regulated by transcription, translation and protein degradation. Transcription largely determines the number of mRNA molecules, whereas the balance of mRNA translation and protein degradation is important for the regulation of protein homeostasis. Upon encountering stress, a cell needs to quickly alter its proteome, thus, as a type of primary response to stress, translation often becomes attenuated. Consequently, mRNAs that are no longer engaged in translation are frequently stored in processing bodies (P bodies) (Parker and Sheth, 2007). P bodies consist of the decapping enzymes Dcp1 and Dcp2, the helicase Dhh1, activators of decapping – such as Pat1, Scd6, Edc3 and the Lsm1–7 complex – and the 5′-3′ exonuclease Xrn1 (Parker and Sheth, 2007). In addition to this basic assortment of P body components, an ever-growing list of proteins associated with P bodies has been reported (Jain and Parker, 2013; Mitchell et al., 2013; Parker and Sheth, 2007).

Growth & Development, Biozentrum, University of Basel, Klingelbergstrasse 70, 4056 Basel, Switzerland.

*Author for correspondence (anne.spang@unibas.ch)

Received 2 September 2013; Accepted 4 February 2014

To date, P bodies have been reported to be involved in mRNA decapping, nonsense-mediated decay, translational repression, mRNA storage and other RNA related functions (Parker and Sheth, 2007). The transcripts that are stored in P bodies are in a dynamic exchange with the pool of mRNAs undergoing translation and can either be degraded or be bound by ribosomes for translation.

P bodies are not the only ribonucleoprotein (RNP) structures that are formed upon stress. Numerous stress conditions also promote the formation of stress granules. Stress granules are mainly composed of stalled translation initiation components and are sites of mRNA storage. The analysis of the different RNP structures is complicated by the fact that numerous factors are found in both types of granules, such as the exonuclease Xrn1 (Buchan and Parker, 2009). In addition, mRNA can traverse from P bodies into stress granules and vice versa (Buchan et al., 2008). Moreover, P bodies and stress granules are found in close contact to each other, which might facilitate the transfer of components and mRNA.

In yeast, 5′-to-3′ decay of mRNA appears to be the major direction of mRNA degradation (Muhlrad et al., 1995; Shoemaker and Green, 2012). Once the cell encounters stress, P bodies become visible by microscopy, which is thought to occur through the aggregation of P body components that are, presumably, bound to mRNA. These aggregates are, nevertheless, highly dynamic and can dissolve either upon adaptation of the cell to the stressor or when the stress ceases to exist (Brengues et al., 2005; Teixeira and Parker, 2007). Depending upon the stress that is encountered, the size and number of P bodies varies. For example, glucose starvation induces a few relatively large foci, whereas high salt and high Ca^{2+} cause the formation of smaller but more numerous P bodies (Brengues et al., 2005; Kilchert et al., 2010). The reason for the different responses is not clear. It has to be noted, however, that glucose starvation can only be remedied by the addition of a good carbon source, whereas cells can adapt to stresses such as high salt (Ashe et al., 2000; Brengues et al., 2005). As a consequence, P bodies that form under such stress disassemble after adaptation (Kilchert et al., 2010).

P bodies are found in close proximity to, and might even be physically linked to, the endoplasmic reticulum (ER) (Kilchert et al., 2010). To determine whether P bodies are physically linked to the ER, we aimed to identify proteins that bind to P body components. The peripheral ER proteins Scp160 and Bfr1 were identified as interacting proteins of P bodies. The association of Scp160 and Bfr1 with polysomes prompted us to test whether Scp160 and Bfr1 might play a role in P body formation. Our results suggest that Bfr1 and Scp160 act independently as negative regulators of P body formation at the ER. Moreover, our data imply that Scp160 is required for the correct assembly of P bodies.

Journal of Cell Science

Journal of Cell Science (2014) 127, 1992–2004 doi:10.1242/jcs.142083

RESULTS

Screen for novel P-body-interacting proteins at the endoplasmic reticulum

We have shown previously that P bodies are localized in close proximity to ER membranes (Kilchert et al., 2010). In order to identify potential ER-localized interaction partners of P body components, we employed tandem affinity purification after crosslinking with the P body components Dcp2 and Scd6, which are part of the 5′UTR- and the 3′UTR-associated complexes of P bodies, respectively. We chose a crosslinking approach because P bodies are highly dynamic, and their interaction with the ER could be transient (Teixeira and Parker, 2007). We also opted for a stringent method and, therefore, selected the HBH tag for the purification scheme. The HBH tag consists of a biotinylation sequence, which is flanked by two His_6 peptides, allowing tandem purification under denaturing conditions (Tagwerker et al., 2006).

The temperature-sensitive *arf1-11* mutation in the small GTPase Arf1p causes the formation of numerous P bodies at the restrictive temperature (Kilchert et al., 2010). Cultures of *arf1-11* mutants expressing chromosomally tagged Dcp2–HBH or Scd6–HBH and wild-type cells were shifted to 37℃ for 1 h to induce P bodies. Protein complexes were crosslinked *in vivo*, extracted from membrane pellets that had been enriched for ER membranes, and purified over Ni-NTA and streptavidin beads under denaturing conditions. The proteins were digested, and the peptides analyzed by mass spectrometry. This approach was successful because we could identify P body components in our purification scheme (Table 1). In addition, proteins were identified that were neither present in the untagged wild-type control nor in other HBH purifications for unrelated baits that have been performed by our group (Ritz et al., 2014). Those proteins present only in the Dcp2–HBH or Scd6–HBH sample, or in both samples, were considered for further analysis (Table 1).

Bfr1 and Scp160 are newly identified P-body-interacting proteins at the ER

Three of the proteins identified in the tandem affinity purifications were ER-associated proteins – Bfr1, Scp160 and Cdc48. Cdc48 is a AAA-ATPase that is involved in homotypic membrane fusion during karyogamy, and in the extraction and retro-translocation of polypeptides from the ER that are destined for degradation by the proteasome (Hitchcock et al., 2001; Latterich et al., 1995; Schuberth and Buchberger, 2005). The function of Cdc48 in ER-associated degradation might mean that it also transmits a signal to induce P body formation under ER stress conditions. We decided, however, to focus on the two other proteins Scp160 and Bfr1. Scp160 is an mRNA-binding protein that, together with Bfr1, associates with actively translating polysomes at the ER (Lang et al., 2001). Loss of Scp160 causes mislocalization of the asymmetrically localized *ASH1* mRNA (Irie et al., 2002; Trautwein et al., 2004) and *SRO7* mRNA after pheromone treatment (Gelin-Licht et al., 2012). Bfr1 has been identified as a multicopy suppressor of brefeldinA-induced lethality (Jackson and Képès, 1994). However, the molecular function of Bfr1 is still unknown.

First, we established whether Scp160 and Bfr1 are still associated with the ER at 37℃, the temperature at which we performed the crosslink. To this end, we appended both Scp160 and Bfr1 chromosomally with a GFP tag in strains that expressed the ER marker Sec63 that had been tagged with red fluorescent protein (RFP). Both proteins remained associated with the ER, irrespective of the temperature (23℃ or 37℃) or the strain background (wild-type or *arf1-11*) (Fig. 1).

Because we used a crosslinking approach to detect proteins that interact with P body components, we wanted to ensure that Scp160 and Bfr1 were not just localized in the vicinity of P bodies and therefore caught in the complex, and that Scp160 and Bfr1 were also able to interact with P body components in the absence of crosslinking agents. 3× FLAG tagged Scp160 co-immunoprecipitated Dcp2 that had been tagged with nine repeats of a Myc epitope (9Myc), irrespective of whether the cells were stressed by glucose starvation, high intracellular Ca^{2+} or unstressed (Fig. 2A,B). The association of Bfr1 with Dcp2 was detected to a lower extent, and the levels were more variable, indicating that Dcp2 might interact primarily with Scp160 rather than with Bfr1. Given that Scp160 is an RNA-binding protein and interacts with the machinery that stores and decays mRNAs, we next tested whether the interaction between Scp160 and Dcp2 was dependent on mRNA. Indeed, treatment of yeast lysates with RNase strongly reduced the amount of co-immunoprecipitated Dcp2 (Fig. 2C).

To explore the possibility that other P body components could also interact with Scp160 and/or Bfr1, we repeated the

Table 1. Proteins identified by HBH-purification

Found only in Dcp2-HBH	Found only in Scd6-HBH	Found in both purifications
Nog1	**Sbp1**	**Dcp2**
Hta1	*Eap1*	**Xrn1**
Atp1	*Not1*	**Edc3**
Cdc48**	Rps12	**Scd6**
	Hef3	*Bfr1***
	Hsp12	**Dhh1**
	Tif5	Tef4
	*Scp160***	Sti1
	Yra1	*Pab1*
	Tif3	Cpr1
	Psp2	*Nam7*
	Lsm5	**Pat1**
	Lsm2	Def1
	Dcp1	Vma13
		Hsp26
		Mpg1

Bold formatting indicates P body components, italic formatting indicates RNA-related function, ** indicates ER association.

Journal of Cell Science (2014) 127, 1992–2004 doi:10.1242/jcs.142083

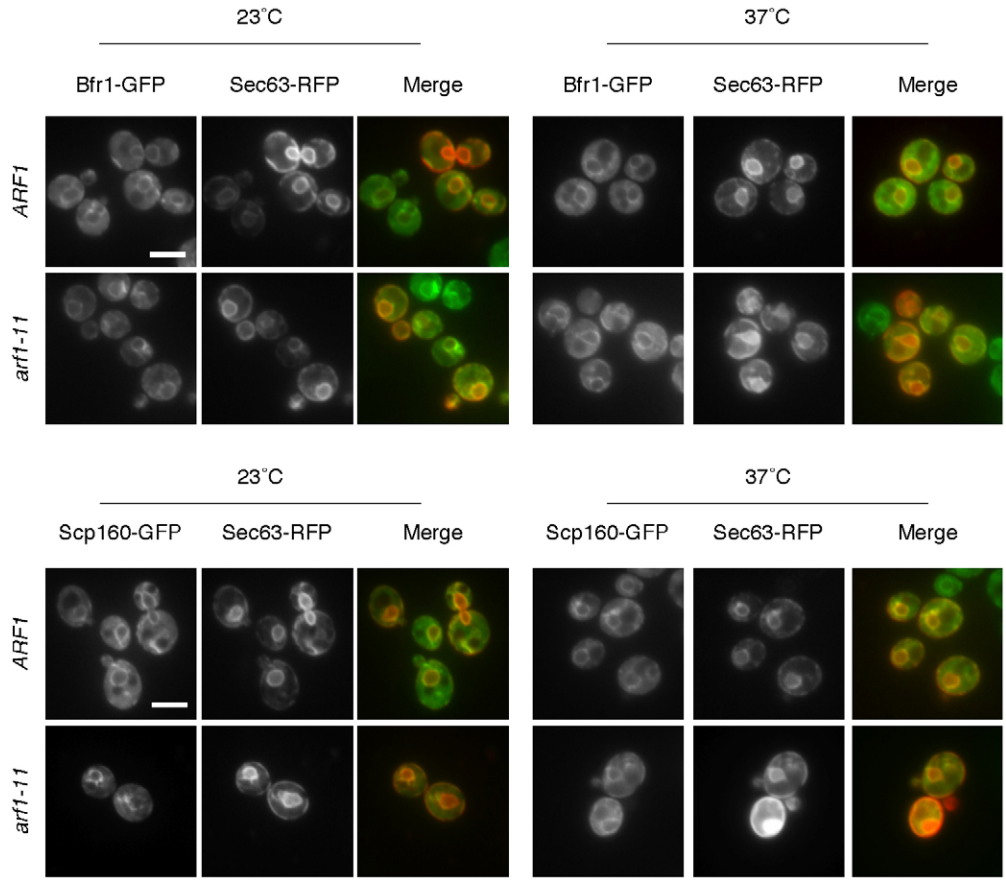

Fig. 1. Bfr1p and Scp160 are identified as potential interacting proteins of P bodies at the ER. Bfr1 and Scp160 localize to the ER. Strains were created in which Bfr1 and Scp160 were chromosomally tagged with GFP (in a background of ARF1 or *arf1-11*, the latter induces P body formation at the restrictive temperature). These strains were then transformed with a plasmid encoding Sec63–RFP (red) to label the ER. Cells were observed at 23°C and after a 1 h shift to 37°C to mimic the conditions that had been used for the HBH purification. At both temperatures, Bfr1–GFP and Scp160–GFP (green) localized to ER membranes. Scale bars: 5 μm.

immunoprecipitations and probed for Pat1 and Edc3, both of which had been tagged with six repeats of the HA epitope (Pat1–6HA and Edc3–6HA, respectively), without stress or under glucose starvation (Fig. 2D). Similar to Dcp2, Pat1 and Edc3 were part of a complex that was associated with, at least, Scp160–FLAG. In all cases, the stress seemed to slightly, but consistently, increase the interaction of Scp160 with these P body components. By contrast, Scd6–6HA was not co-immunoprecipitated with Scp160–FLAG (Fig. 2D). The ability of Scp160 to interact with P body components appeared to be independent of stress, indicating that induction of stress is not a prerequisite for the interaction of P body components with Scp160. Because Dcp2 and Pat1 play a more prominent role in P body assembly (Teixeira and Parker, 2007), our data suggest that at least partially assembled P bodies could be present on actively translating ribosomes. We conclude that Scp160 is a newly identified mRNA-dependent protein that interacts with P body components at the ER.

Scp160 and Bfr1 are not required for the localization of P bodies to the ER

P bodies localize in close proximity to the ER (Kilchert et al., 2010). Therefore, we asked whether Scp160 and Bfr1 are required for P body localization at the ER. Dcp2–9Myc-positive structures were detected by immunoelectron microscopy as being in close proximity to the ER in both the *Δbfr1* and *Δscp160* cells, or in the wild type, when shifted to 37°C (Fig. 3A). The distribution of the Dcp2–9Myc signal, which was suggestive of a ring-like globular structure, was similar in both strains. We then used a biochemical assay to investigate further the results of the ultrastructural analysis. We have shown previously that Dcp2–9Myc co-migrates with ER membranes in a sucrose gradient (Kilchert et al., 2010); here, the association of Dcp2 with the ER was not drastically altered in either of the deletion strains (Fig. 3B) – similar amounts of Dcp2–9Myc floated at the 0% to 40% sucrose interface. Our data demonstrate that neither Scp160 nor Bfr1 are essential for the recruitment of Dcp2 to ER membranes.

P body components co-fractionate with polysomes independently of Scp160 or Bfr1

Bfr1 and Scp160 have been shown to be associated with polysomes (Lang et al., 2001), therefore, we asked whether P body components could be recruited to polysomes. We fractionated polysomes from wild-type, *Δscp160*, *Δbfr1* and *Δbfr1 Δscp160* cells on a sucrose gradient and subjected the polysome fractions to immunoblot analysis. As previously observed (Baum et al., 2004; Li et al., 2003), we did not find a significant change in the polysome profile or an increase in the 80S monosome fraction in any of the strains, which would be indicative of translation attenuation (Fig. 4A). In all cases, Dcp2–9Myc and Scd6–6HA were detected in the polysome fraction (Fig. 4A); thus, association of P body components with the polysomes is independent of Bfr1 and Scp160.

P bodies were not induced in the wild-type cells under the growth conditions that were used for the experiment; therefore, our data indicate that P body components are associated with polysomes during translation in normal logarithmically growing cells. We noticed that Dcp2–9Myc was detected as a double band by immunoblotting, and that, in the fractions of the *Δscp160 Δbfr1* polysome profile, the upper band was strongly reduced.

Journal of Cell Science (2014) 127, 1992–2004 doi:10.1242/jcs.142083

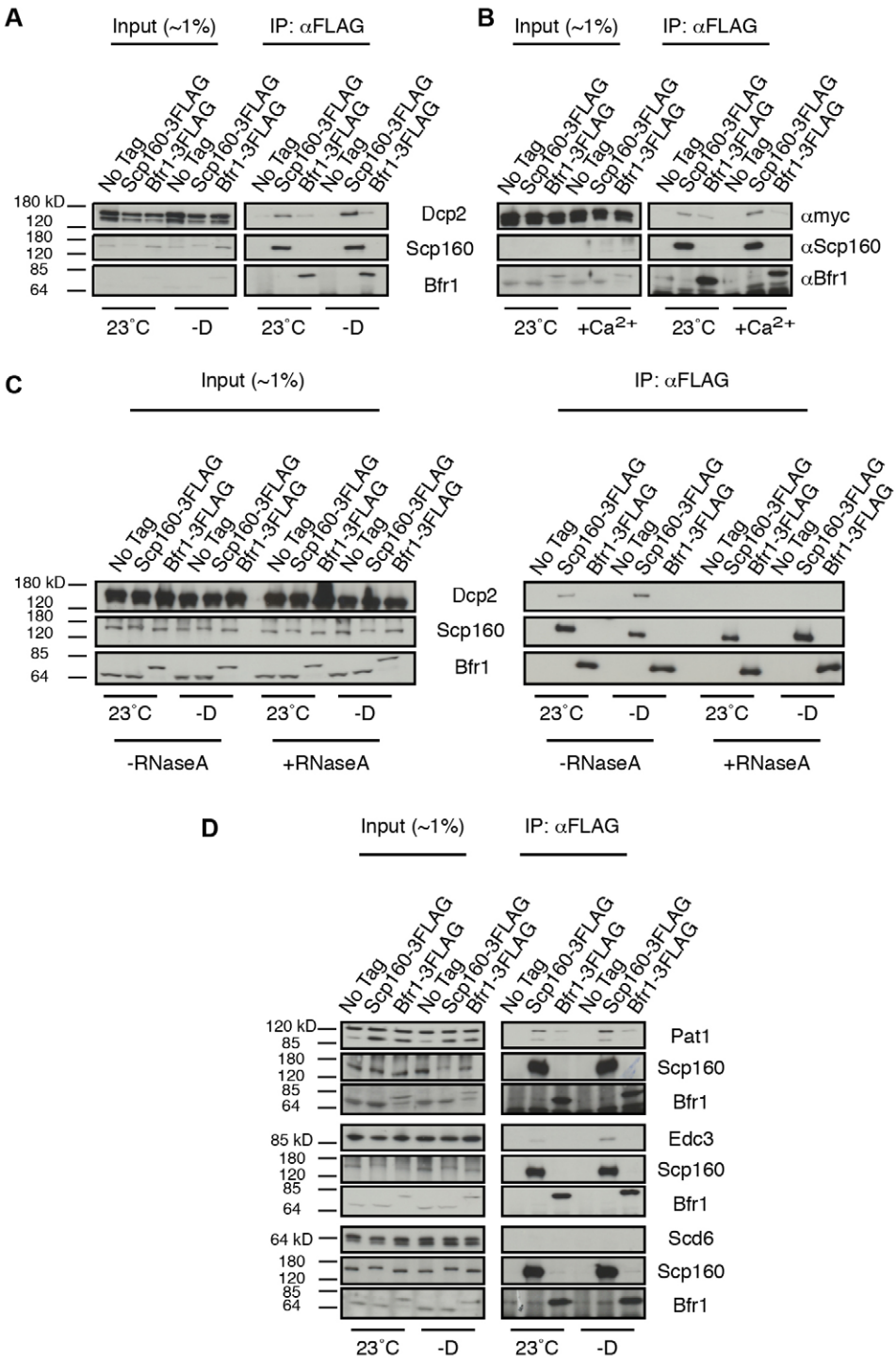

Fig. 2. Scp160 associates with P body components independently of stress. (A) Scp160 associates with Dcp2 independently of glucose starvation. Co-immunoprecipitation experiments were performed using an antibody against the FLAG peptide and lysates from strains that had been chromosomally tagged with Scp160–3FLAG or Bfr1–3FLAG. All strains also expressed Dcp2–9Myc. Where indicated, cells were subjected to starvation for 10 min (−D) before the immunoprecipitation (IP). Dcp2–9Myc co-precipitated with Scp160–3FLAG in both conditions. A weak precipitation of Dcp2–9Myc with Bfr1–FLAG was sometimes observed. (B) Ca^{2+} stress does not affect the Scp160–Dcp2 association. Cells were treated with 200 mM $CaCl_2$ for 10 min ($+Ca^{2+}$) and then a 5 min washout in rich media without $CaCl_2$ was performed before lysate preparation. Under stressed and unstressed conditions, Dcp2–9Myc co-immunoprecipitated with Scp160–3FLAG. (C) The association of Scp160 with Dcp2 is lost in the absence of RNA. To determine if RNA was needed for the interaction between Scp160 and Dcp2, strains were treated as in A and then subjected to treatment with RNaseA for 1 h before immunoprecipitation. Upon RNaseA treatment, the association of Dcp2–9Myc with Scp160–3FLAG was no longer observed under either condition. (D) Scp160 associates with P body components. Pat1, Edc3 or Scd6 were chromosomally appended with a 6HA tag. The strains were treated as in A. Scp160–3FLAG was able to precipitate Pat1–6HA and Edc3–6HA under both conditions but did not precipitate Scd6-6HA.

Thus, we tested whether the double band represented different phosphorylation states. Phosphorylation of Dcp2 has been previously reported, but no band shift in SDS gels had been observed (Yoon et al., 2010). Treatment of the gradient fractions with alkaline phosphatase caused the double band to collapse into the lower molecular weight band (Fig. 4B). These data suggest that phosphorylated and non-phosphorylated forms of Dcp2 are present on polysomes.

P bodies are present on ER membranes, and Scp160 and Bfr1 are enriched on ER-associated polysomes; yet, we used total yeast lysate for the polysome profiles. It is conceivable that P body components associate with the ER-bound polysomes in an Scp160–Bfr1-dependent manner. Moreover, the phosphorylated and dephosphorylated forms of Dcp2 might segregate between membrane-bound and soluble polysomes. To test these hypotheses, we recorded the polysome profiles of membrane and soluble fractions (supplementary material Fig. S1). Immunoblotting of the gradient fractions revealed that P body components could bind to soluble and membrane-associated polysomes (Fig. 4A). Interestingly, the ER-associated polysome pool was enriched for the phosphorylated form of Dcp2 (Fig. 4A). Phosphorylation of Dcp2 has been reported to be required for its accumulation in P

Journal of Cell Science (2014) 127, 1992–2004 doi:10.1242/jcs.142083

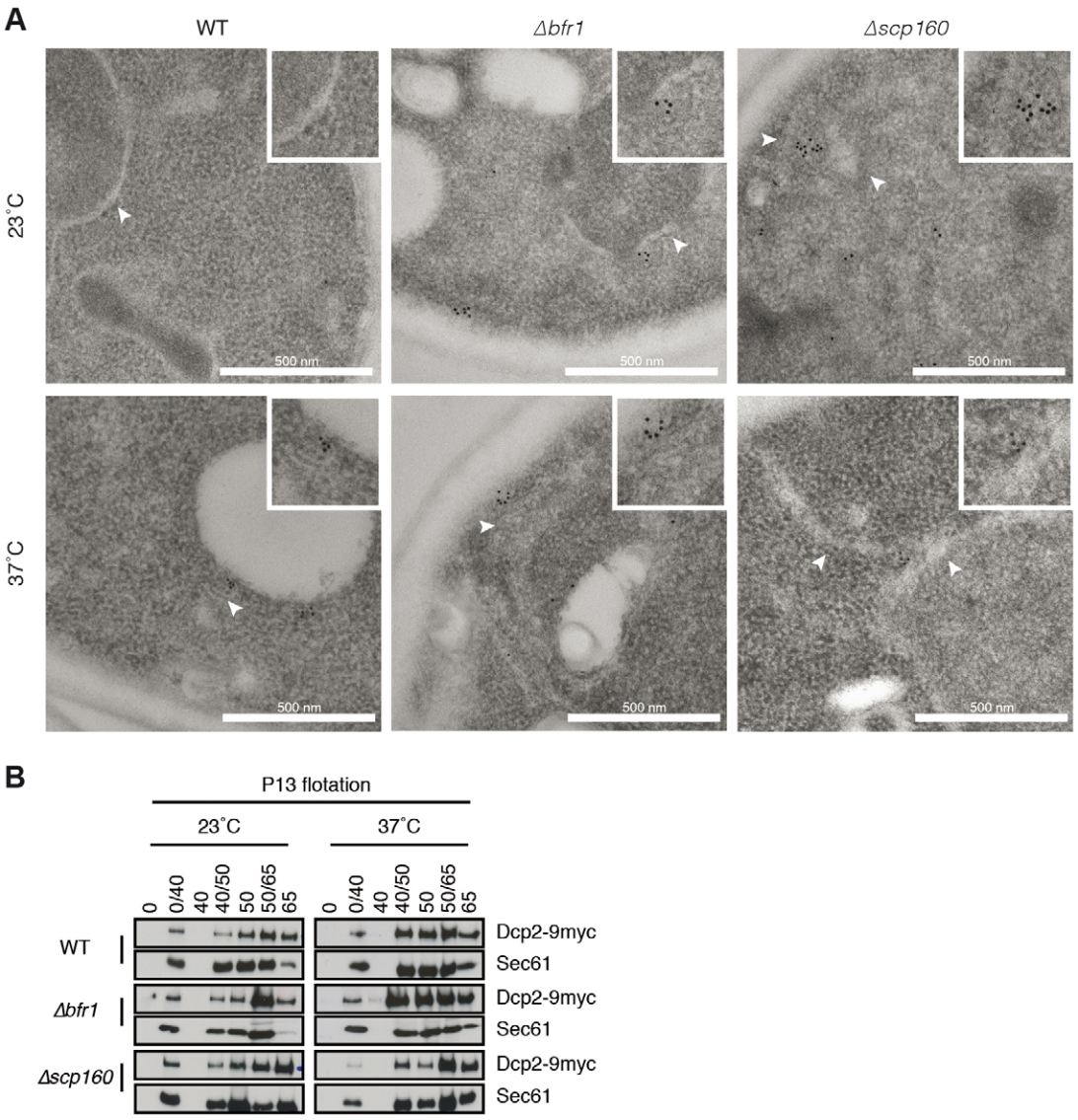

Fig. 3. Loss of *BFR1* or *SCP160* does not impair P body association with the ER. (A) P bodies remain in close proximity to ER membranes in *Δbfr1* and *Δscp160* cells. Cells that expressed Dcp2–9Myc, in which *BFR1* or *SCP160* had been deleted, were grown at 23˚C and then shifted for 1 h to 37˚C. A wild-type (WT) control is also shown. Cells were fixed and prepared for immunoelectron microscopy. Dcp2–9Myc was visualized by using gold particles. Scale bars: 500 nm. The insets are a 2× magnification of the area where the gold particles were found. White arrowheads indicate ER membranes. (B) Dcp2 associates with ER membranes in the absence of *BFR1* or *SCP160*. Wild-type, *Δbfr1* and *Δscp160* yeast cells expressing Dcp2–9Myc were shifted to 37˚C for 1 h. Lysates were prepared, and a pellet was formed from a 13,000 ***g*** centrifugation (P13) and corresponding supernatant fraction (S13). The pellet was subjected to buoyant density centrifugation. In all conditions, a portion of Dcp2–9Myc fractionated with the ER marker Sec61p at the 0% to 40% sucrose interface (0/40).

bodies (Yoon et al., 2010), which is consistent with the notion that P bodies are associated with ER membranes (Kilchert et al., 2010). Notably, the amount of phosphorylated Dcp2 was reduced in the soluble polysome pool in *Δscp160 Δbfr1* cells, indicating that Scp160 and Bfr1 together are required to maintain the Dcp2 phosphorylation state. Taken together, our data demonstrate that P body components are associated with polysomes and suggest that phosphorylated Dcp2 preferentially binds to membrane-associated polysomes.

Loss of Bfr1 or Scp160 induces the formation of multiple Dcp2-positive structures

The immunoelectron microscopy analysis revealed that, unlike in wild-type cells, in the *Δscp160* and *Δbfr1* strains, Dcp2–9Myc-positive structures were readily observed under normal non-stress growth conditions (Fig. 3A, 23˚C). This observation led us to determine whether P bodies form in the mutant strains without any stress being applied at the normal growth temperature. Indeed, when we visualized Dcp2–GFP in the *Δbfr1* and *Δscp160* strains, and in the *Δbfr1 Δscp160* double mutant, we found a large increase in the number of P bodies compared with the wild-type cells, which typically contained 0–2 P bodies per cell (Fig. 5A,B; supplementary material Fig. S2A). Importantly, this increase in Dcp2-positive structures was restricted to normal growth conditions. Shifting the mutant cells to 37˚C, which causes a mild temperature stress – as indicated by the small increase in P body number in wild-type cells – reduced the number of the Dcp2-positive structures in the mutant strains to below even that of the

Journal of Cell Science (2014) 127, 1992–2004 doi:10.1242/jcs.142083

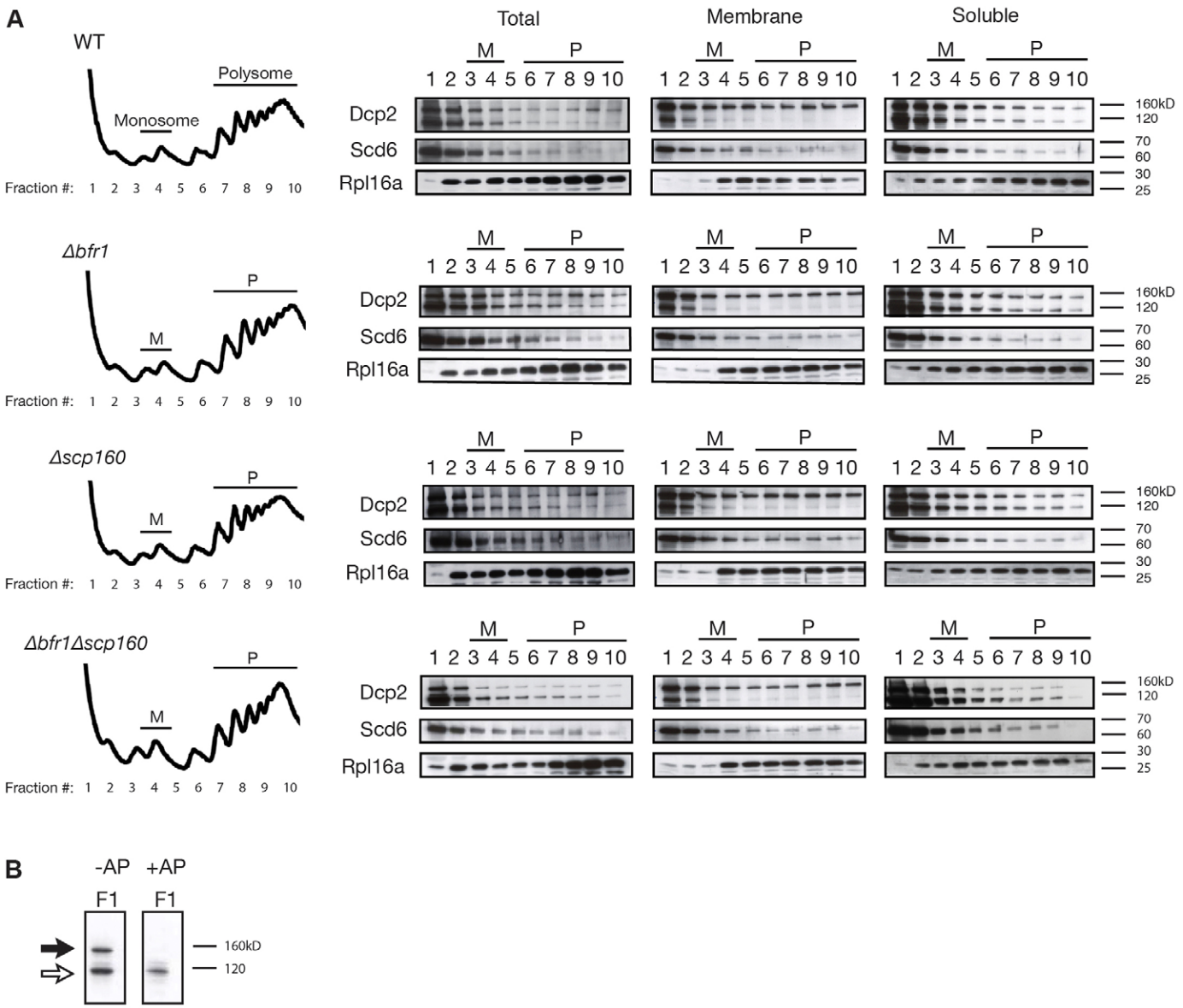

Fig. 4. P body components associate with polysomes. (A) Loss of *BFR1* or *SCP160* does not cause translation attenuation or dissociation of P body components. Cells were grown to mid-log phase and subjected to polysome profile analysis. Despite the large increase in P body number in *Δbfr1*, *Δscp160 and Δbfr1Δscp160* cells at 23˚C, there was no attenuation in translation. Polysome profile fractions from total lysate, lysates containing membrane-associated polysomes or soluble polysomes were TCA precipitated, analyzed by SDS-PAGE and blotted for the P body proteins Dcp2–9Myc and Scd6–6HA or the ribosomal protein Rpl16a. The charts on the left show recordings of polysome profiles. M indicates monosome and P polysome fractions. In all cases, a portion of Dcp2–9Myc and Scd6–6HA were found to associate with polysomes. M, monosome; P, polysome. (B) The double bands observed for Dcp2–9Myc is the result of phosphorylation. Fractions of the polysome profile analysis were subjected to treatment with alkaline phosphatase. Upon alkaline phosphatase treatment, the upper band was lost (black arrow) resulting in only the presence of the lower band (white arrow), indicating that the upper band was due to phosphorylation.

wild type (Fig. 5A,B). We aimed to phenocopy the effect of the *Δscp160* deletion by expressing an Scp160 C-terminal truncation that has been shown previously to compromise Scp160 function (Baum et al., 2004). The removal of the four most-C-terminal K homology (KH) domains induced the formation of multiple Dcp2-positive foci (Scp160 ΔC4, supplementary material Fig. S2B), which is consistent with this truncation having been shown to be hypersensitive to treatment with cycloheximide and the proposed role of Scp160 in translation (Baum et al., 2004). Deletion of either *BFR1* or *SCP160* causes a plethora of phenotypes; therefore, it is possible that the P body phenotype is caused by stress due to extended cultivation of the deletion strains. To rule out this possibility, we replaced the endogenous promoter of *SCP160* and *BFR1* with the inducible MET25 promoter, which is inhibited upon addition of methionine to the growth medium. Under these growth conditions, P body induction was still observed (supplementary material Fig. S2C). Taken together, these data suggest that Scp160 and Bfr1 negatively regulate P body formation under normal growth and stress-free conditions.

Loss of Scp160 or Bfr1 does not induce stress granule formation

Given the increase of P bodies in *Δbfr1* and *Δscp160* cells and that, under certain conditions, P body formation is coupled to

Journal of Cell Science (2014) 127, 1992–2004 doi:10.1242/jcs.142083

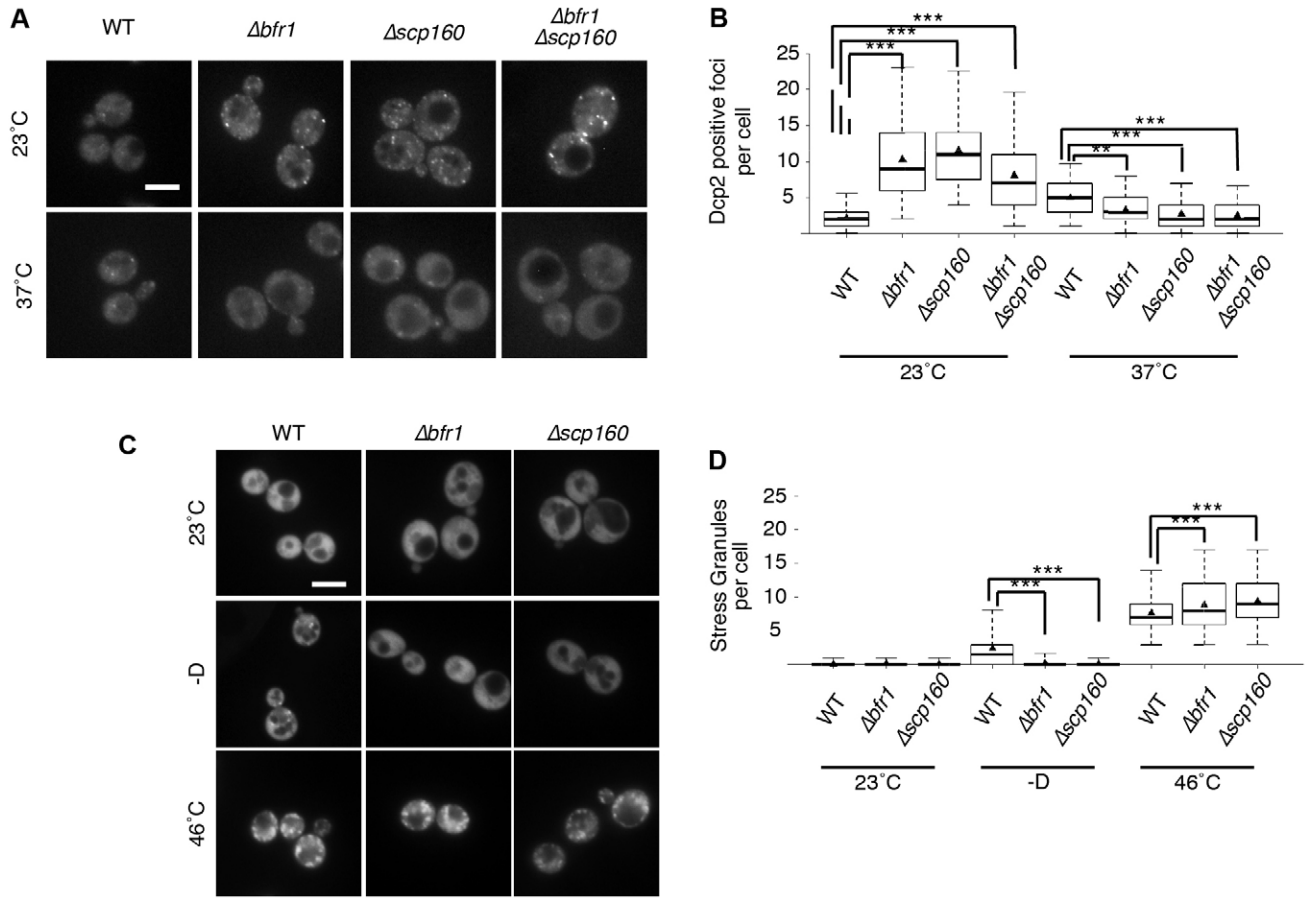

Fig. 5. Loss of *BFR*1 or *SCP*160 increases P body number under normal growth conditions. (A) Increased P body number was observed in *Δbfr1*, *Δscp160* and *Δbfr1Δscp160* cells. Dcp2 was chromosomally tagged and used as a marker for P bodies. Under normal growth conditions at 23˚C in the wild-type (WT) strain 0–2 P bodies were observed. Upon deletion of *BFR1*, *SCP160* or both from the cell, the number of P bodies increased. (B) Quantification of the P body phenotype observed in the wild-type and deletion strains upon temperature shift. A minimum of 200 cells from at least three independent experiments were counted per condition. The size of the box is determined by the 25th and 75th percentiles, the whiskers represent the 5th and 95th percentiles, the horizontal line and the triangle represent the median and mean, respectively. ***$P<0.001$, **$P<0.01$. (C) Stress granules failed to form in *Δbfr1* or *Δscp160* cells under starvation conditions. Wild-type, *Δbfr1* and *Δscp160* cells were transformed with a high copy plasmid expressing the stress granule marker Pub1–mCherry. Cells were grown to mid-log phase at 23˚C then shifted to 46˚C or incubated in rich media lacking a carbon source (−D) for 10 min. (D) Quantification of Pub1-positive foci that were observed under various stresses. ***$P<0.001$. Scale bars: 5 μm.

stress granule formation (Yoon et al., 2010), we next asked whether the number of stress granules is also increased under standard growth conditions in the mutant strains. Stress granule formation has been demonstrated to occur under glucose starvation and under heat stress (Buchan et al., 2008; Grousl et al., 2009). As a marker for stress granule formation, we used the polyU-binding protein Pub1p (Buchan et al., 2008). Indeed, we observed stress granule formation in wild-type cells under both conditions, whereas, in *Δscp160* and *Δbfr1* cells, stress granules were only visible after heat stress (Fig. 5C,D). Thus, Scp160 and Bfr1 might be required for stress granule formation only under certain stresses. Consistently, the *Δbfr1* and *Δscp160* strains did not induce stress granule formation under standard growth conditions (Fig. 5C,D); therefore, the phenotype of P body induction in the *Δbfr1* and *Δscp160* strains is not strictly coupled to stress granule formation.

Overexpression of *SCP160* or *BFR1* rescues the enhanced P body formation phenotype of *Δbfr1* or *Δscp160*, respectively

Bfr1 and Scp160 form a complex at actively translating polysomes, and their localization at the ER is interdependent, nevertheless, they have been shown to have distinct functions (Lang et al., 2001). For example, only Scp160 binds mRNA, and only Bfr1 causes resistance to brefeldinA when overexpressed (Jackson and Képès, 1994; Lang and Fridovich-Keil, 2000; Weber et al., 1997). Moreover, Scp160, rather than Bfr1, bound to the mRNA associated P body components. We, therefore, wondered whether the interaction of Scp160 with Bfr1 is required to prevent P body formation under normal growth conditions, or whether Bfr1 and Scp160 can act independently. To distinguish between these possibilities, we overexpressed *SCP160* and *BFR1* by using the strong *TEF1* promoter in the *Δbfr1* and *Δscp160* strains, respectively. Both genes were also overexpressed, individually, in the wild-type strain. In wild-type cells, the increased expression caused both proteins to also localize to the cytoplasm, indicating that the binding sites at the ER were saturable (Fig. 6A). Overexpression of *BFR1* in *Δscp160* cells, or *SCP160* in *Δbfr1* cells, reduced the number of Dcp2-positive foci to that found in wild-type cells (Fig. 6B,C). This reciprocal rescue was specific because overexpression of the unrelated ArfGAP *GLO3*, under the control of the *TEF1* promoter, did not

Journal of Cell Science (2014) 127, 1992–2004 doi:10.1242/jcs.142083

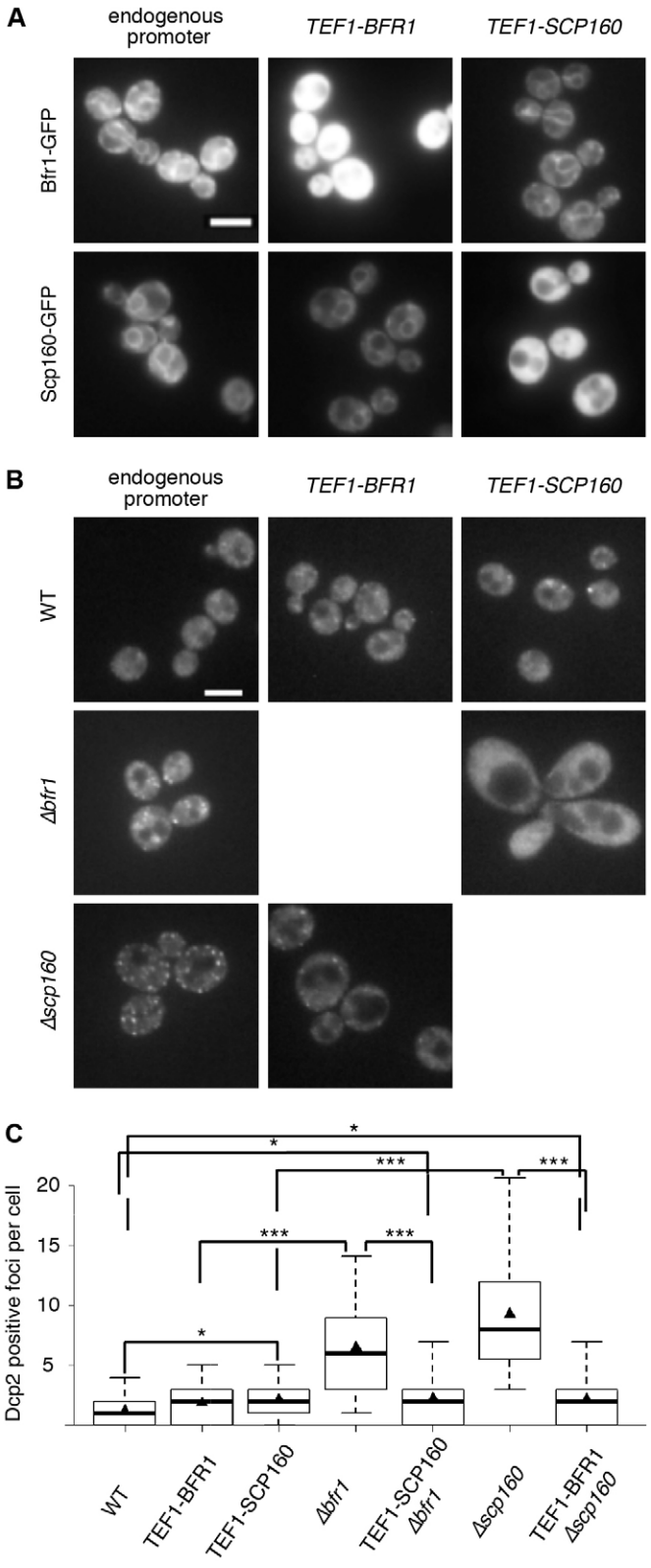

Fig. 6. Overexpression of *SCP160* or *BFR1* rescues the Dcp2-foci phenotype in the reciprocal deletion. (A) Overexpression of Bfr1–GFP or Scp160–GFP led to saturation of ER sites, whereas Bfr1–GFP or Scp 160–GFP remained at the ER in *TEF1-SCP160* or *TEF1-BFR1* cells, respectively. The endogenous promoters of *BFR1* or *SCP160* were chromosomally exchanged for the constitutive *TEF1* promoter and the localization of Bfr1–GFP or Scp160–GFP was observed. (B) Dcp2-positive foci were reduced in *TEF1-SCP160 Δbfr1* or *TEF1-BFR1 Δscp160* strains compared with the deletions alone. *BFR1* or *SCP160* were overexpressed in strains expressing Dcp2–GFP in which either *SCP160* or *BFR1* had been deleted. (C) Quantification of the Dcp2-positive foci in cells shown in B. See Fig. 5B for details on the representation. ***$P<0.001$, *$P<0.05$. Scale bars: 5 μm.

rescue the multiple-P-body phenotype in *Δscp160* or *Δbfr1* strains (supplementary material Fig. S2D); thus, merely increasing the mRNA levels did not rescue the P body phenotype. These data indicate that both Scp160 and Bfr1 are able to independently prevent P body formation under normal growth conditions.

Loss of Scp160 generates pseudo P bodies

So far we have shown that loss of Scp160 and Bfr1 induces Dcp2-positive foci. P bodies are highly dynamic structures in which P body components assemble in an aggregate-like manner, similar to prions. In fact, a number of P body proteins contain prion-like domains (Alberti et al., 2009; Reijns et al., 2008); thus, it would be conceivable that, in the absence of Scp160 or Bfr1, proper P bodies do not form. Given that the formation of P bodies requires the presence of RNA in these structures (Coller and Parker, 2005; Teixeira et al., 2005), we treated cells with cycloheximide, which 'locks' ribosomes onto mRNA and restricts the availability of the mRNA for the formation of P bodies. As expected, treatment of cells with cycloheximide abolished the Dcp2-positive foci in the mutant strains (Fig. 7A), indicating that *Δscp160* and *Δbfr1* cause the appearance of bona fide P bodies.

To expand our results, we determined the localization of three additional P body constituents (Scd6, Edc3 and Dhh1) (Fig. 7B and C). All of the markers formed multiple foci in *Δbfr1* cells, only a few Scd6- or Edc3-positive structures were observed in *Δscp160* cells and Dhh1 did not form foci that would correspond to P-bodies. To demonstrate that the foci formed by the different P body components associated with the same structures, we co-expressed Dcp2–GFP and Edc3–mCherry (supplementary material Fig. S2E). The localizations of the P body components showed extensive overlap, indicating that they are, indeed, present on the same structure. These data indicate that, in *Δbfr1* cells, *bona fide* P bodies are formed in the absence of stress. By contrast, loss of Scp160 led to the formation of aggregates that lacked certain P body components, which we define as pseudo P bodies. Our results suggest that Scp160 might play a role in the assembly of P body proteins. Taken together, our data are consistent with both Bfr1 and Scp160 being negative regulators of P body formation in the absence of stress.

Scp160 and Bfr1 do not repress P body formation under stress

We hypothesized that because Bfr1 and Scp160 associate with actively translating polysomes, both proteins could prevent access of P body components to mRNA during translation. During stress conditions, under which translation is attenuated (Brengues et al., 2005; Kilchert et al., 2010), it is possible that polysomes disassemble and, therefore, that Scp160 and Bfr1 are lost from the mRNA, which means that they cannot protect mRNA and cannot be involved in the control of P body formation. Consequently, the loss of Scp160 or Bfr1 should not affect P body formation under such stress conditions. Upon withdrawal of glucose from wild-type, *Δscp160* or *Δbfr1* cultures, we observed P body induction to a similar extent in wild-type and *Δbfr1* cells (Fig. 7D and E). A small increase in the number of Dcp2-positive

Journal of Cell Science (2014) 127, 1992–2004 doi:10.1242/jcs.142083

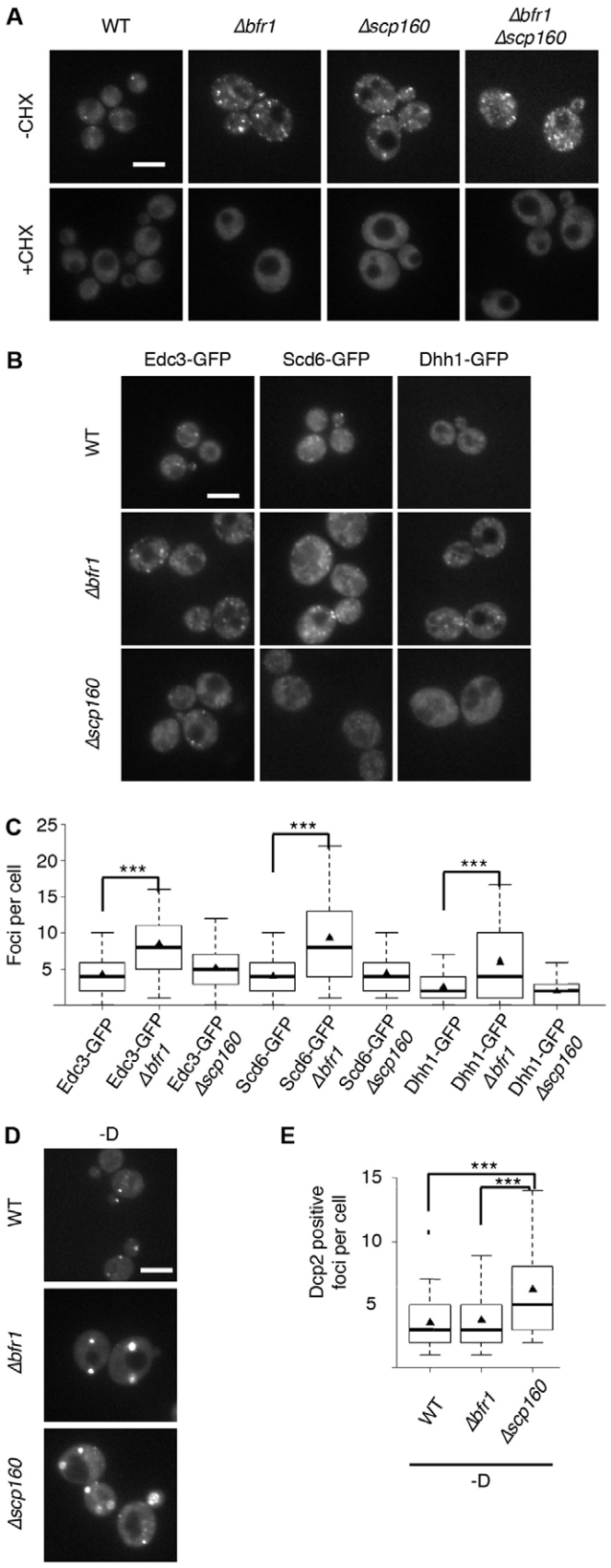

Fig. 7. Pseudo P bodies are formed in *Δscp160* cells. (A) Cycloheximide inhibits the formation of Dcp2-positive foci. Dcp2–GFP expressing cells were grown at 23˚C to mid-log phase and then cycloheximide was added to a final concentration of 100 µg/ml for 10 min before imaging. In all cases, few, if any, Dcp2-positive foci were observed upon addition of cycloheximide, indicating that the Dcp2-containing foci contained RNA. (B) Pseudo P bodies are formed in *Δscp160* cells. To test if the Dcp2 containing foci were bona fide P bodies, either *BFR1* or *SCP160* was deleted from strains that expressed Edc3–GFP, Scd6–GFP or Dhh1–GFP . Although multiple foci were observed in *Δbfr1* cells for all markers, very few foci were observed in *Δscp160* cells. (C) Quantification of the Edc3–GFP-, Scd6–GFP- and Dhh1–GFP-positive foci observed in B. ***$P<0.001$. For a description of the quantification, see Fig. 5B. (D) Starvation induces Dcp2-positive foci. Cells containing Dcp2–GFP were grown to mid-log phase and then incubated in rich medium without a carbon source (−D) for 10 min before imaging. Bright Dcp2-positive foci were observed in wild-type (WT), *Δbfr1* and *Δscp160* cells. In *Δscp160* cells, foci of different sizes were observed. (E) Quantification of the Dcp2–GFP foci observed under conditions of starvation in D. ***$P<0.001$. Scale bars: 5 µm.

structures was observed in the *Δscp160* strain, consistent with a role for Scp160 in the correct assembly of P bodies. A similar result was obtained under heat stress (supplementary material Fig. S3). Our results are consistent with Scp160 and Bfr1 having a negative role on the formation of P bodies, but only in the absence of stress.

DISCUSSION

P body formation is an important process by which eukaryotic cells respond to a plethora of stresses, such as environmental, metabolic and cellular stress. Here, we aimed to understand why P bodies are localized in close proximity to the ER membrane. We find that P body components interact with the polysome-associated mRNA-binding protein Scp160. This interaction exposes the P body components to mRNA molecules as soon as they are released from the polysomes. Thus, the function of Scp160, and its interacting protein Bfr1, is, probably, to keep the P body components in a ‘waiting’ position but, nevertheless, inhibit the formation of P bodies under normal growth and stress-free conditions (Fig. 8). In this model, as soon as the cell encounters stress, the protective function of Scp160 and Bfr1 is lost, and P body components have unrestricted access to mRNAs.

We find that loss of either Bfr1 or Scp160 causes the formation of multiple Dcp2-positive structures. Although both structures contain mRNA, only the Dcp2-positive foci in *Δbfr1* cells appear to be fully assembled P bodies (Fig. 8). In *Δscp160* cells, the Dcp2-positive structures do not contain all of the P body components and, hence, are probably not functional in terms of mRNA decay. Thus, Scp160 appears to play a, perhaps, regulatory role in the correct assembly of P bodies. We assume that this role is more involved in the regulation of the process, because P bodies formed in *Δscp160* strains under glucose starvation and also because stress granules appeared under heat stress.

The association of P body components with polysomes is, perhaps, not surprising. Different laboratories have previously proposed a model of dynamic equilibrium in which P body formation is directly coupled to translation attenuation (Coller and Parker, 2005; Franks and Lykke-Andersen, 2008). The most plausible way to achieve this coupling would be through a direct interaction. In addition, influencing the phosphorylation state of Dcp2 could be a part of the regulation of the dynamic equilibrium. Dcp2 is predominantly in the phosphorylated state on membrane-associated polysomes, whereas the phosphorylated

Journal of Cell Science (2014) 127, 1992–2004 doi:10.1242/jcs.142083

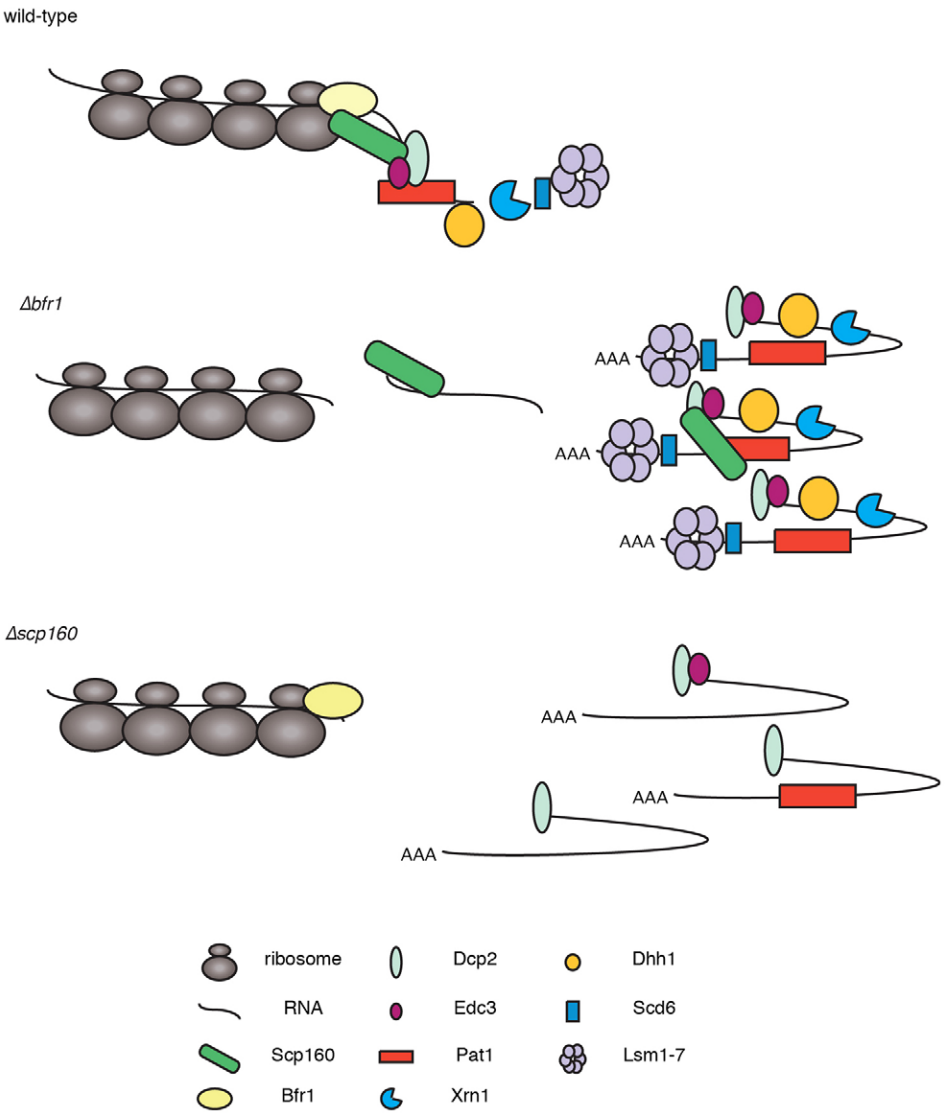

Fig. 8. Scp160 and Bfr1 inhibit P body formation under normal growth conditions. In wild-type cells under normal growth conditions, Scp160 and Bfr1 protect RNA at polysomes. Scp160 interacts with RNA and P body components and leaves P bodies in a 'waiting' position while still inhibiting P body formation. In *Δbfr1* cells, Scp160 is not efficiently recruited to the polysomes and cannot properly protect the RNA, thus, allowing P body components to access RNAs. In *Δscp160*, Bfr1 can, to an extent, be recruited to polysomes, but without Scp160, proper P body assembly cannot occur, leading to the formation of pseudo P bodies.

and non-phosphorylated forms of Dcp2 are present in the soluble pool of polysomes. Phosphorylation of Dcp2 is required for the assembly of P bodies, which might influence the decay of some mRNAs (Yoon et al., 2010). Because P bodies are in close proximity to the ER, the phosphorylation state of Dcp2 might represent a 'primed state' for P body formation. Moreover, the P body components Dhh1 and Pat1 have been shown to be translational repressors, indicating that there might be a feedback mechanism between P bodies and ribosomes (Franks and Lykke-Andersen, 2008; Pilkington and Parker, 2008).

Scp160 and Bfr1 are, most likely, not the only proteins that can restrict the access of P body components to polysome-associated mRNA. Moreover, they are not essential for the association of P body components with polysomes, or the localization of P bodies close to the ER. Still, it is noteworthy that Scp160 is predominantly associated with membrane-bound polysomes (Weber et al., 1997). Thus, it cannot be excluded that Scp160 has some role in P body localization to the ER. It has been established that Scp160 only binds to a subset of mRNAs (Gelin-Licht et al., 2012; Hogan et al., 2008; Li et al., 2003), and a biological role for the mRNA–Scp160 interaction has been demonstrated for *ASH1* mRNA localization and pheromone sensing (Gelin-Licht et al., 2012; Irie et al., 2002; Trautwein et al., 2004). Importantly, Scp160 has been shown to bind *DHH1* mRNA and is required for efficient translation of this message (Li et al., 2003). Thus, Scp160 could be part of a regulatory loop that controls the translation of specific messages. In the case of Dhh1, however, we could not detect a difference in the protein levels in *Δscp160* cells (supplementary material Fig. S4). This role could be regulated by phosphorylation because Scp160 is phosphorylated upon inhibition of the TOR complex by rapamycin, mimicking amino acid starvation (Soulard et al., 2010). In addition, Scp160 is part of a complex that contains Eap1, a negative regulator of translation (Cosentino et al., 2000; Mendelsohn et al., 2003). In fact, the Smy2, Eap1, Scp160, Asc1 (SESA) complex has been shown to act as a translational repressor of the *POM34* mRNA in response to spindle pole body (SPB) duplication defects (Sezen et al., 2009). Pom34 is a component of the nuclear pore complex that plays a role in the insertion of the SPB into the nuclear envelope.

Scp160 appears to have multiple cellular functions – Scp160 controls ploidy (hence the name *S*accharomyces protein *c*ontrolling ploidy) (Wintersberger et al., 1995), it is required for the asymmetric localization of mRNAs (Gelin-Licht et al.,

Journal of Cell Science (2014) 127, 1992–2004 doi:10.1242/jcs.142083

2012; Irie et al., 2002; Trautwein et al., 2004) and is part of a translational repressor complex (Sezen et al., 2009). Scp160 might also act as a signaling platform on ribosomes to control the translation of specific mRNAs (Baum et al., 2004), as it has been shown to act as an effector of a G-protein in the mating response pathway (Guo et al., 2003) and contributes to the regulation of telomere silencing (Marsellach et al., 2006). Furthermore, here, we show that Scp160 negatively regulates P body formation in the absence of stress and might be a novel P body component. How can all of these functions be performed by one protein? Scp160 could be part of different complexes that regulate Scp160 functions and recruit it to the correct site of function; such an adaptor function could be performed by Bfr1. Scp160 requires Bfr1 for efficient polysome association, and Bfr1 might recruit the SESA complex to the SPB (Sezen et al., 2009). However, Bfr1 must have additional functions, besides being an Scp160 interactor because overexpression of *BFR1* in the *Δscp160* strain was sufficient to alleviate the pseudo P body phenotype, and the concomitant loss of *BFR1* and *SCP160* showed a strong reduction of phosphorylated Dcp2 on soluble polysomes. Bfr1 might directly interact with P body components, although with a lower affinity than Scp160. Overexpression of *BFR1* could, potentially, increase its interaction with P body components and maintain the P body components in the 'waiting' position.

In addition, the localization of *ASH1* mRNA at the bud tip is not only dependent on Scp160 but also on Bfr1 and ribosomes (Irie et al., 2002; Trautwein et al., 2004). Thus, it is conceivable that Bfr1 is the adaptor for complexes that are involved in translation activation and repression. Clearly, Scp160 must have other adaptor proteins to fulfill its Bfr1-independent roles as a G protein effector or in the silencing of telomeres.

Scp160 is conserved in species up to human, and the closest homologues are vigilin (also known as HDLBP) and the fragile X syndrome protein FMRP (also known as FMR1) (Currie and Brown, 1999; Weber et al., 1997). Vigilin has been proposed to have a role in cytoplasmic mRNA metabolism in *Drosophila* and human cell lines (Goolsby and Shapiro, 2003) and to protect vitellogenin mRNA from degradation by the mRNA endonuclease PMR-1 in *Xenopus* (Cunningham et al., 2000). In addition, vigilin binds to the mRNA of the proto-oncogene c-fms and inhibits its translation, thereby relieving suppression of breast cancer cell proliferation (Cao et al., 2004; Woo et al., 2011). These functions might be regulated in a similar manner through binding to polysomes, because, akin to Scp160, vigilin binds to ribosomes through its C-terminal tail (Vollbrandt et al., 2004). Furthermore, the second mammalian homologue of Scp160 FMRP binds to a subset of mRNAs, and the I304N mutation, which was first described in an fragile X syndrome (FXS) patient, reduces the association of the protein with mRNAs and polysomes (Ascano et al., 2012; Feng et al., 1997; Siomi et al., 1994). Therefore, it is also conceivable that the function of Scp160 to control the translation of a subset of mRNAs is also conserved in vigilin and FMRP.

MATERIALS AND METHODS

Yeast methods

Standard genetic techniques were used throughout (Sherman, 1991). All modifications were carried out chromosomally, with the exceptions listed below. Chromosomal tagging and deletions were performed as described previously (Knop et al., 1999; Knop et al., 1999; Gueldener et al., 2002; Gueldener et al., 2002). For co-staining of the ER, the cells were transformed with the plasmid pSM1959 (with selectable marker LEU2) carrying Sec63–RFP (kindly provided by Susan Michaelis, Johns Hopkins University, Baltimore, MD). pRP1661 (with selectable marker URA3) encoding Pub1–mCherry and pRP1575 (with selectable marker TRP1) encoding Edc3–mCherry were provided by Roy Parker (University of Colorado, Boulder, CO). The plasmid pMS449 carrying the ΔC4 truncation of Scp160 was obtained from Matthias Seedorf (ZMBH Heidelberg, Germany). The plasmid pTEF-Glo3-FLAG (with selectable marker LEU2) was created through amplification of the *GLO3* gene using the primers Glo3-6F and Glo3-11R (5′-GCAATTTAGGA-TCCAC-ATAGCGACAATGAG-3′ and 5′-GAGAAAATTCTCGAGA-TTTTCTTAAGTAG-3′, respectively) and the resulting fragment was cloned using *Bam*HI and *Xho*I into pcDNA3.1 with a C-terminal FLAG tag.

The C-terminal FLAG tag was obtained through PCR of the plasmid pcDNA3.1+the Glo3-FLAG construct with the primers Glo3-6F and Glo3-10R (5′-GGCAAACTGCAGATGGCTG-3′). The resulting PCR fragment was digested with *Bam*HI and *Pst*I, and ligated into vector p425TEF. The final plasmids were confirmed by sequencing. The strains used in this study are listed in supplementary material Table S1.

HBH-purification

The HBH purification was carried out as previously described by Tagwerker and colleagues (Tagwerker, et al., 2006) with modifications. Cells that expressed Dcp2–HBH or Scd6–HBH were grown to mid-to-late log phase at 23℃ then shifted for 1 h to 37℃. The cells were fixed by adding 37% formaldehyde to a final concentration of 1% and incubating at room temperature for 2 min with gentle agitation. The formaldehyde was quenched for 5 min by the addition of glycine to a final concentration of 1.25 mM. The cells were harvested (4700 ***g*** for 3 min at 4℃), washed in 50 ml ice-cold double distilled H_2O, pooled, sedimented by centrifugation (5 min at 3000 ***g***), flash frozen in liquid nitrogen and stored at −80℃. The cells were thawed and resuspended in 2 ml of buffer 1 (50 mM NaPi pH 8.0, 8M urea, 300 mM NaCl 20 mM imidazole, 0.5% Tween-20) per gram of yeast cell pellet. Per 2 ml screw capped tube containing 500 µl glass beads, 1 ml of the cell suspension was added. Lysis was performed in a FastPrep instrument four times for 45 seconds each at 4℃. The glass beads and cell debris were cleared with a slow spin (1300 ***g*** for 10 min at 4℃), and the supernatant was removed and pooled. The supernatants were spun at 20,000 ***g*** for 15 min at 4℃ and the resulting pellets were resuspended in 500 µl buffer 1 with the addition of 1% Tween-20. 2.5 ml of Ni-NTA slurry that had been washed in buffer 1 was added to the pooled lysates and rotated overnight at room temperature. The tubes were spun at room temperature for 3 min at 2500 ***g*** and washed with 10 ml buffer 1. The tubes were spun as before and a series of 10 ml washes and spins were sequentially performed (buffer 2: 50 mM NaPi pH 6.4, 8 M urea, 300 mM NaCl, 0.5% Tween-20; buffer 3: 50 mM NaPi pH 8.0, 8 M urea, 300 mM NaCl, 0.5% Tween-20, 20 mM imidazole; buffer 4: 50 mM NaPi pH 8.0, 8 M urea, 300 mM NaCl, 0.5% Tween-20, 40 mM imidazole). After the final wash and spin, 4 ml of elution buffer (50 mM NaPi pH 6.4, 8 M urea, 300 mM NaCl, 0.5% Tween-20, 300 mM imidazole) was added and rotated with the beads for 45 min. The beads were spun down as before, the eluate was collected, and the elution step was repeated. 300 µl streptavidin agarose that had been washed in buffer 1 was added to the 8 ml of elute and rotated for 2 h at room temperature. The slurry was then spun as before and washed with 10 ml of buffer 6 (50 mM Tris-HCl pH 8.0, 8 M urea, 300 mM NaCl, 2% SDS). This step was then repeated with 10 ml buffer 7 (50 mM Tris-HCl pH 8.0, 8 M urea, 300 mM NaCl, 0.2% SDS). The final wash was performed in buffer 8 (50 mM Tris-HCl pH 8.0, 8 M urea, 300 mM NaCl) and the streptavidin agarose was resuspended in 1 ml buffer 8. The slurry was then washed three times with 1 ml 50 mM Tris-HCl pH 8.0 with 0.1% SDS, and 50 µl of solution was left in the tube after the final wash. To each tube, 0.25 µl of 1 mg/ml Endoproteinase LysC (ELC) was added, and the tubes were placed at 37℃ with shaking. After 2 h, a further 0.25 µl of 1 mg/ml ELC was added and the tubes were placed at 37℃ overnight with shaking. The tubes were briefly spun down and the supernatant was collected. The beads were extracted twice with of 50 mM Tris-HCl pH 8.0 with 0.1% SDS (in a volume of 200 µl followed by 100 µl). The three samples were pooled and dried in a Speed-Vac concentrator. The peptides were

resuspended in 400 µl BS (85% acetonitrile, 10 mM ammonium acetate with formic acid pH 3.5) and loaded twice on a HILIC TopTip PolyLC spin column (PolyLC) that had been equilibrated three times with 50 µl ES (5% acetonitrile, 10 mM ammonium acetate with formic acid pH 3.5) and three times with 50 µl BS. The column was washed three times with 50 µl BS and the peptides were eluted four times with 25 µl ES. All elutions were pooled and dried in a Speed-Vac concentrator. The peptides were then resuspended in 50 µl of 50 mM NH_4HCO_3 and subjected to trypsin digest with 0.5 µl 1 mg/ml trypsin (Promega) for 6 h at 37℃. Mass spectrometric analysis was performed using LC-MS/MS (Orbitrap).

Fluorescence microscopy

Cells were grown in yeast extract peptone dextrose (YPD) medium to early-log phase and then either shifted to 37℃ for 1 h or subjected to various stresses, as indicated. The cells were spun at 3000 ***g*** for 3 min and resuspended in Hartwell's complete (HC) medium and immobilized on concanavalin-A-coated slides. For strains harboring the pTEF-Glo3-FLAG plasmid, the cells were grown in HC medium that lacked leucine. In the methionine experiments, cells were grown at 30℃ in YPD containing 100 µg/ml methionine for 72 h and maintained at an OD_{600} of between 0.2 and 1.0 through continuous dilution.

Fluorescence was monitored with an Axiocam mounted on an Axioplan 2 fluorescence microscope (Carl Zeiss, Oberkochen, Germany) by using Axiovision software. Image processing was performed using Image J and Adobe Photoshop CS5 (San Jose, CA). For counting, a minimum of 200 cells from at least three independent experiments was counted per condition. In the quantification graphs, the size of the box is determined by the 25th and 75th percentiles, the whiskers represent the 5th and 95th percentiles, the lines and the triangles mark the median and the mean, respectively.

Immunoelectron microscopy

Cells expressing Dcp2–9Myc were grown to early-log phase at 23℃ and then shifted to 37℃ for 1 h. The cells were fixed and treated for immunoelectron microscopy as described previously (Prescianotto-Baschong and Riezman, 2002). Secondary antibodies against goat anti-rabbit IgG that had been coupled to 10-nm gold particles (BBInternational, Cardiff, United Kingdom) were used to detect the binding of polyclonal rabbit antibodies that recognise Myc (Abcam, Cambridge, MA).

Immunoprecipitations

Immunoprecipitations were performed similarly as described previously (Sezen et al., 2009). Twenty OD_{600} units of logarithmically growing cells that had been grown in YPD and subjected to the various stresses, as indicated, were disrupted with glass beads in 300 µl of immunoprecipitation buffer [50 mM triethanolamine pH 6.0, 150 mM KCl, 5 mM EDTA, 5 mM EGTA, protease inhibitor tablet (Roche), 1 mM PMSF and 1 mM benzamidine]. The lysates were incubated with 1% Triton X-100 for 10 min at 4℃, and the extracts were cleared by centrifugation (3000 ***g*** for 10 min at 4℃). An aliquot was removed that served as the input control, and the remainder of the extract was incubated with a monoclonal antibody against FLAG peptide (M2, Invitrogen) and magnetic bead slurry (Dynal) for 2.5 h at 4℃. The beads were washed three times with immunoprecipitation buffer containing 0.1% Triton X-100. The beads were resuspended in sample buffer and analyzed by immunoblotting.

For the RNase A treated samples, after the extracts had been cleared by centrifugation, they were treated with 40 U of RNase inhibitor (Promega) or 1 µg/µl RNase A and incubated for 1 h at 4℃. The extracts were then spun for 3 min at 3000 ***g***, and the supernatant was used for the immunoprecipitation as described above.

Antibodies

Antibodies were used to detect the following epitope tags and proteins: Myc (9E10, 1:1000, Sigma-Aldrich), hemagglutinin (HA11, 1:1000, Covance, Princeton, NJ), Scp160 (1:1000), Bfr1 (1:1000), Rpl16a (1:1500, a gift from Michael N. Hall, Biozentrum, Basel, Switzerland) and Sec61 (1:10,000, a gift from Martin Spiess, Biozentrum, Basel, Switzerland).

Flotation of P bodies

Flotation of ER membranes was performed as described previously (Schmid et al., 2006). The equivalent of 50 OD_{600} units was converted into sphereoplasts at 37℃ and lysed by Dounce homogenization in 3 ml lysis buffer [20 mM HEPES in KOH, pH 7.6, 100 mM sorbitol, 100 mM KAc, 5 mM $Mg(Ac)_2$, 1 mM EDTA, 1 mM dithiothreitol, 100 µg/ml cycloheximide, protease inhibitors]. After the removal of cellular debris (5 min, 300 ***g***), the membranes were pelleted by centrifugation (10 min, 13,000 ***g***), resuspended in 2 ml lysis buffer containing 50% sucrose and layered on top of 2 ml 65% sucrose in lysis buffer. Two additional 5 ml and 2 ml cushions (40% and 0% sucrose) were layered on top. The step gradient was spun in a TST41.14 rotor for 16 h at 28,000 ***g***. After centrifugation, 1 ml fractions were collected from each of the cushions and the interfaces, and were then precipitated with trichloroacetic acid (TCA). The samples were analyzed by SDS-PAGE and immunoblotting.

Polysome profile analysis

Preparations of polysomes were performed as described previously (de la Cruz et al., 1997) on 4–47% sucrose gradients that had been prepared using a Gradient Master (Nycomed Pharma, Westbury, NY). Gradient analysis was performed using a gradient fractionator (Labconco, Kansas City, MO) and the Ächta FPLC system (GE Healthcare) and continuously monitored at A_{254}. Fractions were precipitated with 10% TCA, separated using SDS-PAGE and analyzed by western blotting.

Acknowledgements

We thank Cornelia Kilchert (Biozentrum, University Basel), Roy Parker, Matthias Seedorf, Michael N. Hall, Martin Spiess, Paul Jenö, Suzette Moes, Ian G Macara for reagents. Paul Jenö and Suzette Moes (Biozentrum, University of Basel) are acknowledged for the mass spectrometric analysis of the HBH purifications. Ian G. Macara is acknowledged for critically reading the manuscript.

Competing interests

The authors declare no competing interests.

Author contributions

J.W. and A.S. conceived the study; J.W., C.W., C.P.-B., A.F.E. and A.S. performed the experiments and analyzed the data; A.S. wrote the manuscript; all authors provided comments on the manuscript.

Funding

This work was supported by Werner-Siemens Fellowships (to J.W. and C.W.), the Human Frontiers Science Program [grant number RGP0031/2009-C], the Swiss National Science Foundation [grant number 31003A_141207] and the University of Basel (to A.S.).

Supplementary material

Supplementary material available online at
http://jcs.biologists.org/lookup/suppl/doi:10.1242/jcs.142083/-/DC1

References

Alberti, S., Halfmann, R., King, O., Kapila, A. and Lindquist, S. (2009). A systematic survey identifies prions and illuminates sequence features of prionogenic proteins. *Cell* **137**, 146-158.

Ascano, M., Jr, Mukherjee, N., Bandaru, P., Miller, J. B., Nusbaum, J. D., Corcoran, D. L., Langlois, C., Munschauer, M., Dewell, S., Hafner, M. et al. (2012). FMRP targets distinct mRNA sequence elements to regulate protein expression. *Nature* **492**, 382-386.

Ashe, M. P., De Long, S. K. and Sachs, A. B. (2000). Glucose depletion rapidly inhibits translation initiation in yeast. *Mol. Biol. Cell* **11**, 833-848.

Baum, S., Bittins, M., Frey, S. and Seedorf, M. (2004). Asc1p, a WD40-domain containing adaptor protein, is required for the interaction of the RNA-binding protein Scp160p with polysomes. *Biochem. J.* **380**, 823-830.

Brengues, M., Teixeira, D. and Parker, R. (2005). Movement of eukaryotic mRNAs between polysomes and cytoplasmic processing bodies. *Science* **310**, 486-489.

Buchan, J. R. and Parker, R. (2009). Eukaryotic stress granules: the ins and outs of translation. *Mol. Cell* **36**, 932-941.

Buchan, J. R., Muhlrad, D. and Parker, R. (2008). P bodies promote stress granule assembly in Saccharomyces cerevisiae. *J. Cell Biol.* **183**, 441-455.

Cao, W. M., Murao, K., Imachi, H., Yu, X., Abe, H., Yamauchi, A., Niimi, M., Miyauchi, A., Wong, N. C. and Ishida, T. (2004). A mutant high-density lipoprotein receptor inhibits proliferation of human breast cancer cells. *Cancer Res.* **64**, 1515-1521.
Coller, J. and Parker, R. (2005). General translational repression by activators of mRNA decapping. *Cell* **122**, 875-886.
Cosentino, G. P., Schmelzle, T., Haghighat, A., Helliwell, S. B., Hall, M. N. and Sonenberg, N. (2000). Eap1p, a novel eukaryotic translation initiation factor 4E-associated protein in Saccharomyces cerevisiae. *Mol. Cell. Biol.* **20**, 4604-4613.
Cunningham, K. S., Dodson, R. E., Nagel, M. A., Shapiro, D. J. and Schoenberg, D. R. (2000). Vigilin binding selectively inhibits cleavage of the vitellogenin mRNA 3′-untranslated region by the mRNA endonuclease polysomal ribonuclease 1. *Proc. Natl. Acad. Sci. USA* **97**, 12498-12502.
Currie, J. R. and Brown, W. T. (1999). KH domain-containing proteins of yeast: absence of a fragile X gene homologue. *Am. J. Med. Genet.* **84**, 272-276.
de la Cruz, J., Iost, I., Kressler, D. and Linder, P. (1997). The p20 and Ded1 proteins have antagonistic roles in eIF4E-dependent translation in Saccharomyces cerevisiae. *Proc. Natl. Acad. Sci. USA* **94**, 5201-5206.
Feng, Y., Absher, D., Eberhart, D. E., Brown, V., Malter, H. E. and Warren, S. T. (1997). FMRP associates with polyribosomes as an mRNP, and the I304N mutation of severe fragile X syndrome abolishes this association. *Mol. Cell* **1**, 109-118.
Franks, T. M. and Lykke-Andersen, J. (2008). The control of mRNA decapping and P-body formation. *Mol. Cell* **32**, 605-615.
Gelin-Licht, R., Paliwal, S., Conlon, P., Levchenko, A. and Gerst, J. E. (2012). Scp160-dependent mRNA trafficking mediates pheromone gradient sensing and chemotropism in yeast. *Cell Rep.* **1**, 483-494.
Goolsby, K. M. and Shapiro, D. J. (2003). RNAi-mediated depletion of the 15 KH domain protein, vigilin, induces death of dividing and non-dividing human cells but does not initially inhibit protein synthesis. *Nucleic Acids Res.* **31**, 5644-5653.
Grousl, T., Ivanov, P., Frýdlová, I., Vasicová, P., Janda, F., Vojtová, J., Malínská, K., Malcová, I., Nováková, L., Janosková, D. et al. (2009). Robust heat shock induces eIF2alpha-phosphorylation-independent assembly of stress granules containing eIF3 and 40S ribosomal subunits in budding yeast, Saccharomyces cerevisiae. *J. Cell Sci.* **122**, 2078-2088.
Gueldener, U., Heinisch, J., Koehler, G. J., Voss, D. and Hegemann, J. H. (2002). A second set of loxP marker cassettes for Cre-mediated multiple gene knockouts in budding yeast. *Nucleic Acids Res.* **30**, e23.
Guo, M., Aston, C., Burchett, S. A., Dyke, C., Fields, S., Rajarao, S. J., Uetz, P., Wang, Y., Young, K. and Dohlman, H. G. (2003). The yeast G protein alpha subunit Gpa1 transmits a signal through an RNA binding effector protein Scp160. *Mol. Cell* **12**, 517-524.
Hitchcock, A. L., Krebber, H., Frietze, S., Lin, A., Latterich, M. and Silver, P. A. (2001). The conserved npl4 protein complex mediates proteasome-dependent membrane-bound transcription factor activation. *Mol. Biol. Cell* **12**, 3226-3241.
Hogan, D. J., Riordan, D. P., Gerber, A. P., Herschlag, D. and Brown, P. O. (2008). Diverse RNA-binding proteins interact with functionally related sets of RNAs, suggesting an extensive regulatory system. *PLoS Biol.* **6**, e255.
Irie, K., Tadauchi, T., Takizawa, P. A., Vale, R. D., Matsumoto, K. and Herskowitz, I. (2002). The Khd1 protein, which has three KH RNA-binding motifs, is required for proper localization of ASH1 mRNA in yeast. *EMBO J.* **21**, 1158-1167.
Jackson, C. L. and Képès, F. (1994). BFR1, a multicopy suppressor of brefeldin A-induced lethality, is implicated in secretion and nuclear segregation in Saccharomyces cerevisiae. *Genetics* **137**, 423-437.
Jain, S. and Parker, R. (2013). The discovery and analysis of P Bodies. *Adv. Exp. Med. Biol.* **768**, 23-43.
Kilchert, C., Weidner, J., Prescianotto-Baschong, C. and Spang, A. (2010). Defects in the secretory pathway and high Ca2+ induce multiple P-bodies. *Mol. Biol. Cell* **21**, 2624-2638.
Knop, M., Siegers, K., Pereira, G., Zachariae, W., Winsor, B., Nasmyth, K. and Schiebel, E. (1999). Epitope tagging of yeast genes using a PCR-based strategy: more tags and improved practical routines. *Yeast* **15**, 963-972.
Lang, B. D. and Fridovich-Keil, J. L. (2000). Scp160p, a multiple KH-domain protein, is a component of mRNP complexes in yeast. *Nucleic Acids Res.* **28**, 1576-1584.
Lang, B. D., Li Am, Black-Brewter, H. D. and Fridovich-Keil, J. L. (2001). The brefeldin A resistance protein Bfr1p is a component of polyribosome-associated mRNP complexes in yeast. *Nucleic Acids Res.* **29**, 2567-2574.
Latterich, M., Fröhlich, K. U. and Schekman, R. (1995). Membrane fusion and the cell cycle: Cdc48p participates in the fusion of ER membranes. *Cell* **82**, 885-893.
Li, A. M., Watson, A. and Fridovich-Keil, J. L. (2003). Scp160p associates with specific mRNAs in yeast. *Nucleic Acids Res.* **31**, 1830-1837.
Marsellach, F. X., Huertas, D. and Azorín, F. (2006). The multi-KH domain protein of Saccharomyces cerevisiae Scp160p contributes to the regulation of telomeric silencing. *J. Biol. Chem.* **281**, 18227-18235.
Mendelsohn, B. A., Li, A. M., Vargas, C. A., Riehman, K., Watson, A. and Fridovich-Keil, J. L. (2003). Genetic and biochemical interactions between SCP160 and EAP1 in yeast. *Nucleic Acids Res.* **31**, 5838-5847.
Mitchell, S. F., Jain, S., She, M. and Parker, R. (2013). Global analysis of yeast mRNPs. *Nat. Struct. Mol. Biol.* **20**, 127-133.
Muhlrad, D., Decker, C. J. and Parker, R. (1995). Turnover mechanisms of the stable yeast PGK1 mRNA. *Mol. Cell. Biol.* **15**, 2145-2156.
Parker, R. and Sheth, U. (2007). P bodies and the control of mRNA translation and degradation. *Mol. Cell* **25**, 635-646.
Pilkington, G. R. and Parker, R. (2008). Pat1 contains distinct functional domains that promote P-body assembly and activation of decapping. *Mol. Cell. Biol.* **28**, 1298-1312.
Prescianotto-Baschong, C. and Riezman, H. (2002). Ordering of compartments in the yeast endocytic pathway. *Traffic* **3**, 37-49.
Reijns, M. A., Alexander, R. D., Spiller, M. P. and Beggs, J. D. (2008). A role for Q/N-rich aggregation-prone regions in P-body localization. *J. Cell Sci.* **121**, 2463-2472.
Ritz, A. M., Trautwein, M., Grassinger, F. and Spang, A. (2014). The prion-like domain in the exomer-dependent cargo Pin2 serves as a trans-Golgi retention motif. *Cell Rep.* doi: 10.1016/j.celrep.2014.02.026. [Epub ahead of print].
Schmid, M., Jaedicke, A., Du, T. G. and Jansen, R. P. (2006). Coordination of endoplasmic reticulum and mRNA localization to the yeast bud. *Curr. Biol.* **16**, 1538-1543.
Schuberth, C. and Buchberger, A. (2005). Membrane-bound Ubx2 recruits Cdc48 to ubiquitin ligases and their substrates to ensure efficient ER-associated protein degradation. *Nat. Cell Biol.* **7**, 999-1006.
Sezen, B., Seedorf, M. and Schiebel, E. (2009). The SESA network links duplication of the yeast centrosome with the protein translation machinery. *Genes Dev.* **23**, 1559-1570.
Sherman, F. (1991). Getting started with yeast. *Methods Enzymol.* **194**, 3-21.
Shoemaker, C. J. and Green, R. (2012). Translation drives mRNA quality control. *Nat. Struct. Mol. Biol.* **19**, 594-601.
Siomi, H., Choi, M., Siomi, M. C., Nussbaum, R. L. and Dreyfuss, G. (1994). Essential role for KH domains in RNA binding: impaired RNA binding by a mutation in the KH domain of FMR1 that causes fragile X syndrome. *Cell* **77**, 33-39.
Soulard, A., Cremonesi, A., Moes, S., Schütz, F., Jenö, P. and Hall, M. N. (2010). The rapamycin-sensitive phosphoproteome reveals that TOR controls protein kinase A toward some but not all substrates. *Mol. Biol. Cell* **21**, 3475-3486.
Tagwerker, C., Flick, K., Cui, M., Guerrero, C., Dou, Y., Auer, B., Baldi, P., Huang, L. and Kaiser, P. (2006). A tandem affinity tag for two-step purification under fully denaturing conditions: application in ubiquitin profiling and protein complex identification combined with in vivo cross-linking. *Mol. Cell. Proteomics* **5**, 737-748.
Teixeira, D. and Parker, R. (2007). Analysis of P-body assembly in Saccharomyces cerevisiae. *Mol. Biol. Cell* **18**, 2274-2287.
Teixeira, D., Sheth, U., Valencia-Sanchez, M. A., Brengues, M. and Parker, R. (2005). Processing bodies require RNA for assembly and contain nontranslating mRNAs. *RNA* **11**, 371-382.
Trautwein, M., Dengjel, J., Schirle, M. and Spang, A. (2004). Arf1p provides an unexpected link between COPI vesicles and mRNA in Saccharomyces cerevisiae. *Mol. Biol. Cell* **15**, 5021-5037.
Vollbrandt, T., Willkomm, D., Stossberg, H. and Kruse, C. (2004). Vigilin is co-localized with 80S ribosomes and binds to the ribosomal complex through its C-terminal domain. *Int. J. Biochem. Cell Biol.* **36**, 1306-1318.
Weber, V., Wernitznig, A., Hager, G., Harata, M., Frank, P. and Wintersberger, U. (1997). Purification and nucleic-acid-binding properties of a Saccharomyces cerevisiae protein involved in the control of ploidy. *Eur. J. Biochem.* **249**, 309-317.
Wintersberger, U., Kühne, C. and Karwan, A. (1995). Scp160p, a new yeast protein associated with the nuclear membrane and the endoplasmic reticulum, is necessary for maintenance of exact ploidy. *Yeast* **11**, 929-944.
Woo, H. H., Yi, X., Lamb, T., Menzl, I., Baker, T., Shapiro, D. J. and Chambers, S. K. (2011). Posttranscriptional suppression of proto-oncogene c-fms expression by vigilin in breast cancer. *Mol. Cell. Biol.* **31**, 215-225.
Yoon, J. H., Choi, E. J. and Parker, R. (2010). Dcp2 phosphorylation by Ste20 modulates stress granule assembly and mRNA decay in Saccharomyces cerevisiae. *J. Cell Biol.* **189**, 813-827.

Table S1: Yeast strains used in this study

Strain	Designation	Genotype	Reference
YPH499	WT	*MAT a ade2-101 his3-200 leu2-1 lys2-801 trp-63 ura3-52*	Sikorski and Hieter, 1989
NYY0-1	ARF1	*MAT a ade2::ARF1::ADE2 arf1::HIS3 arf2::HIS3 ura3 lys2 trp1 his3 leu2*	Yahara et al., 2001
NYY11-1	*arf1-11*	*MAT a ade2::arf1-11::ADE2 arf1::HIS3 arf2::HIS3 ura3 lys2 trp1 his3 leu2*	Yahara et al., 2001
YAS2501	Dcp2-HBH	*MAT a ade2::ARF1::ADE2 arf1::HIS3 arf2::HIS3 ura3 lys2 trp1 his3 leu2 DCP2::DCP2-HBH-kanMX4*	This study
YAS2502	*arf1-11* Dcp2-HBH	*MAT a ade2::arf1-11::ADE2 arf1::HIS3 arf2::HIS3 ura3 lys2 trp1 his3 leu2 DCP2::DCP2-HBH-kanMX4*	This study
YAS3240	Scd6-HBH	*MAT a ade2::ARF1::ADE2 arf1::HIS3 arf2::HIS3 ura3 lys2 trp1 his3 leu2 SCD6::SCD6-HBH-TRP1*	This study
YAS3257	*arf1-11* Scd6-HBH	*MAT a ade2::arf1-11::ADE2 arf1::HIS3 arf2::HIS3 ura3 lys2 trp1 his3 leu2 SCD6::SCD6-HBH-TRP1*	This study
YAS1031A	Dcp2-GFP	*MAT a ade2::ARF1::ADE2 arf1::HIS3 arf2::HIS3 ura3 lys2 trp1 his3 leu2 DCP2::DCP2-yEGFP-kanMX4*	This study
YAS1271	Bfr1-GFP	*MAT a ade2::ARF1::ADE2 arf1::HIS3 arf2::HIS3 ura3 lys2 trp1 his3 leu2 BFR1::BFR1-yEGFP-kanMX4*	This study
YAS1184	Scp160-GFP	*MAT a ade2::ARF1::ADE2 arf1::HIS3 arf2::HIS3 ura3 lys2 trp1 his3 leu2 SCP160::SCP160- yEGFP-kanMX4*	This study
YAS1272	*arf1-11* Bfr1-GFP	*MAT a ade2::arf1-11::ADE2 arf1::HIS3 arf2::HIS3 ura3 lys2 trp1 his3 leu2 BFR1::BFR1-yEGFP-kanMX4*	This study
YAS1185	*arf1-11* Scp160-GFP	*MAT a ade2::arf1-11::ADE2 arf1::HIS3 arf2::HIS3 ura3 lys2 trp1 his3 leu2 SCP160::SCP160-yEGFP-kanMX4*	This study
YAS3135	Dcp2-GFP Δ*bfr1*	*MAT a ade2::ARF1::ADE2 arf1::HIS3 arf2::HIS3 ura3 lys2 trp1 his3 DCP2::DCP2-yEGFP-kanMX4 bfr1::LEU2*	This study
YAS3136	Dcp2-GFP Δ*scp160*	*MAT a ade2::ARF1::ADE2 arf1::HIS3 arf2::HIS3 ura3 lys2 trp1 his3 leu2 DCP2::DCP2-yEGFP-kanMX4 scp160::URA3*	This study
YAS3137	Dcp2-GFP Δ*bfr1*Δ*scp160*	*MAT a ade2::ARF1::ADE2 arf1::HIS3 arf2::HIS3 ura3 lys2 trp1 his3 leu2 DCP2::DCP2-yEGFP-kanMX4 bfr1::LEU2 scp160::URA3*	This study
YAS2238	Edc3-GFP	*MAT a ade2::ARF1::ADE2 arf1::HIS3 arf2::HIS3 ura3 lys2 his3 leu2 EDC3::EDC3-yEGFP-TRP1*	This study
YAS2867	Edc3-GFP Δ*bfr1*	*MAT a ade2::ARF1::ADE2 arf1::HIS3 arf2::HIS3 ura3 lys2 his3 leu2 EDC3::EDC3-yEGFP-TRP1 bfr1::URA3*	This study
YAS2778	Edc3-GFP Δ*scp160*	*MAT a ade2::ARF1::ADE2 arf1::HIS3 arf2::HIS3 ura3 lys2 his3 leu2 EDC3::EDC3-yEGFP-TRP1 scp160::URA3*	This study
YAS1153	Dhh1-GFP	*MAT a ade2::ARF1::ADE2 arf1::HIS3 arf2::HIS3 ura3 lys2 trp1 his3 leu2 DHH1::DHH1-yEGFP-kanMX4*	This study
YAS2878	Dhh1-GFP Δ*bfr1*	*MAT a ade2::ARF1::ADE2 arf1::HIS3 arf2::HIS3 ura3 lys2 trp1 his3 leu2 DHH1::DHH1-yEGFP-kanMX4 bfr1::URA3*	This study
YAS2782	Dhh1-GFP Δ*scp160*	*MAT a ade2::ARF1::ADE2 arf1::HIS3 arf2::HIS3 ura3 lys2 trp1 his3 leu2 DHH1::DHH1-yEGFP-kanMX4 scp160::URA3*	This study
YAS2315	Scd6-GFP	*MAT a ade2::ARF1::ADE2 arf1::HIS3 arf2::HIS3 ura3 lys2 trp1 his3 leu2 SCD6::SCD6-yEGFP-kanMX4*	This study
YAS2819	Scd6-GFP Δ*bfr1*	*MAT a ade2::ARF1::ADE2 arf1::HIS3 arf2::HIS3 ura3 lys2 trp1 his3 leu2 SCD6::SCD6-yEGFP-kanMX4 bfr1::URA3*	This study
YAS2783	Scd6-GFP Δ*scp160*	*MAT a ade2::ARF1::ADE2 arf1::HIS3 arf2::HIS3 ura3 lys2 trp1 his3 leu2 SCD6::SCD6-yEGFP-kanMX4 scp160::URA3*	This study
YAS1294	Dcp2-9myc	*MAT a ade2::ARF1::ADE2 arf1::HIS3 arf2::HIS3 ura3 lys2 trp1 his3 leu2 DCP2::DCP2-9myc-TRP1*	This study

YAS2880	Dcp2-9myc *Δbfr1*	*MAT a ade2::ARF1::ADE2 arf1::HIS3 arf2::HIS3 ura3 lys2 trp1 his3 leu2 DCP2::DCP2-9myc-TRP1 bfr1::URA3*	This study
YAS2881	Dcp2-9myc *Δscp160*	*MAT a ade2::ARF1::ADE2 arf1::HIS3 arf2::HIS3 ura3 lys2 trp1 his3 leu2 DCP2::DCP2-9myc-TRP1 scp160::URA3*	This study
YAS3113	Dcp2-9myc Scp160-3FLAG	*MAT a ade2::ARF1::ADE2 arf1::HIS3 arf2::HIS3 ura3 lys2 trp1 his3 leu2 DCP2::DCP2-9myc--kanMX4 SCP160::SCP160-3FLAG-TRP1*	This study
YAS3112	Dcp2-9myc Bfr1-3FLAG	*MAT a ade2::ARF1::ADE2 arf1::HIS3 arf2::HIS3 ura3 lys2 trp1 his3 leu2 DCP2::DCP2-9myc--kanMX4 BFR1::BFR1-3FLAG-TRP1*	This study
YAS3330	Dcp2-9myc Scp160-3FLAG Pat1-6HA	*MAT a ade2::ARF1::ADE2 arf1::HIS3 arf2::HIS3 ura3 lys2 trp1 his3 leu2 DCP2::DCP2-9myc--kanMX4 SCP160::SCP160-3FLAG-TRP1 PAT1::PAT1-6HA-hphNT1*	This study
YAS3814	Dcp2-9myc Scp160-3FLAG Edc3-6HA	*MAT a ade2::ARF1::ADE2 arf1::HIS3 arf2::HIS3 ura3 lys2 trp1 his3 leu2 DCP2::DCP2-9myc--kanMX4 SCP160::SCP160-3FLAG-TRP1 EDC3::EDC3-6HA-hphNT1*	This study
YAS3815	Dcp2-9myc Scp160-3FLAG Scd6-6HA	*MAT a ade2::ARF1::ADE2 arf1::HIS3 arf2::HIS3 ura3 lys2 trp1 his3 leu2 DCP2::DCP2-9myc--kanMX4 SCP160::SCP160-3FLAG-TRP1) SCD6::SCD6-6HA-hphNT1*	This study
YAS3816	Dcp2-9myc Bfr1-3FLAG Pat1-6HA	*MAT a ade2::ARF1::ADE2 arf1::HIS3 arf2::HIS3 ura3 lys2 trp1 his3 leu2 DCP2::DCP2-9myc--kanMX4 BFR1::BFR1-3FLAG-TRP1 PAT1::PAT1-6HA-hphNT1*	This study
YAS3817	Dcp2-9myc Bfr1-3FLAG Edc3-6HA	*MAT a ade2::ARF1::ADE2 arf1::HIS3 arf2::HIS3 ura3 lys2 trp1 his3 leu2 DCP2::DCP2-9myc--kanMX4 BFR1::BFR1-3FLAG-TRP1 EDC3::EDC3-6HA-hphNT1*	This study
YAS3818	Dcp2-9myc Bfr1-3FLAG Scd6-6HA	*MAT a ade2::ARF1::ADE2 arf1::HIS3 arf2::HIS3 ura3 lys2 trp1 his3 leu2 DCP2::DCP2-9myc--kanMX4 BFR1::BFR1-3FLAG-TRP1 SCD6::SCD6-6HA-hphNT1*	This study
YAS3236	Dcp2-GFP TEF1-Bfr1	*MAT a ade2::ARF1::ADE2 arf1::HIS3 arf2::HIS3 ura3 lys2 trp1 his3 leu2 DCP2::DCP2-yEGFP-kanMX4 BFR1:: natNT2-TEF1-BFR1*	This study
YAS3242	TEF1-Bfr1-GFP	*MAT a ade2::ARF1::ADE2 arf1::HIS3 arf2::HIS3 ura3 lys2 trp1 his3 leu2 BFR1::natNT2-TEF1-BFR1-yEGFP-kanMX4*	This study
YAS3241A	Scp160-GFP TEF1-BFR1	*MAT a ade2::ARF1::ADE2 arf1::HIS3 arf2::HIS3 ura3 lys2 trp1 his3 leu2 SCP160::SCP160-yEGFP BFR1:: natNT2-TEF1-BFR1*	This study
YAS3237	Dcp2-GFP TEF1-SCP160	*MAT a ade2::ARF1::ADE2 arf1::HIS3 arf2::HIS3 ura3 lys2 trp1 his3 leu2 DCP2::DCP2-yEGFP-kanMX4 SCP160 natNT2-TEF1-SCP160*	This study
YAS3243	Bfr1-GFP TEF1-SCP160	*MAT a ade2::ARF1::ADE2 arf1::HIS3 arf2::HIS3 ura3 lys2 trp1 his3 leu2 BFR1::BFR1-yEGFP SCP160:: natNT2-TEF1-SCP160*	This study
YAS3241	TEF1-Scp160-GFP	*MAT a ade2::ARF1::ADE2 arf1::HIS3 arf2::HIS3 ura3 lys2 trp1 his3 leu2 SCP160:: natNT2-TEF1-SCP160*	This study
YAS3239	Dcp2-GFP Δ*bfr1* TEF1-SCP160	*MAT a ade2::ARF1::ADE2 arf1::HIS3 arf2::HIS3 ura3 lys2 trp1 his3 leu2 DCP2::DCP2-yEGFP-kanMX4 SCP160:: natNT2-TEF1-SCP160 bfr1::loxp::ura3::loxp*	This study
YAS3238	Dcp2-GFP Δ*scp160* TEF1-BFR1	*MAT a ade2::ARF1::ADE2 arf1::HIS3 arf2::HIS3 ura3 lys2 trp1 his3 leu2 DCP2::DCP2-yEGFP-kanMX4 BFR1:: natNT2-TEF1-BFR1 scp160::loxp::ura3::loxp*	This study
YAS3789	Dcp2-GFP Δ*bfr1*	*MAT a ade2::ARF1::ADE2 arf1::HIS3 arf2::HIS3 ura3 lys2 trp1 his3 leu2 DCP2::DCP2-yEGFP-kanMX4 bfr1::loxp::ura3::loxp*	This study
YAS3790	Dcp2-GFP Δ*scp160*	*MAT a ade2::ARF1::ADE2 arf1::HIS3 arf2::HIS3 ura3 lys2 trp1 his3 leu2 DCP2::DCP2-yEGFP-kanMX4*	This study

		scp160::loxp::ura3::loxp	
YAS4074	Dcp2-9myc Scd6-6HA Δ*bfr1*	*MAT a ade2::ARF1::ADE2 arf1::HIS3 arf2::HIS3 ura3 lys2 trp1 his3 leu2 DCP2::DCP2-9myc-TRP1 SCD6::SCD6-6HA-hphNT1 bfr1::LEU2*	This study
YAS4075	Dcp2-9myc Scd6-6HA Δ*scp160*	*MAT a ade2::ARF1::ADE2 arf1::HIS3 arf2::HIS3 ura3 lys2 trp1 his3 leu2 DCP2::DCP2-9myc-TRP1 SCD6::SCD6-6HA-hphNT1 scp160::URA3*	This study
YAS4076	Dcp2-9myc Scd6-6HA Δ*bfr1*Δ*scp160*	*MAT a ade2::ARF1::ADE2 arf1::HIS3 arf2::HIS3 ura3 lys2 trp1 his3 leu2 DCP2::DCP2-9myc-TRP1 SCD6::SCD6-6HA-hphNT1 bfr1::LEU2 scp160::URA3*	This study
YAS4047	Dcp2-GFP MET25-Bfr1	*MAT a ade2::ARF1::ADE2 arf1::HIS3 arf2::HIS3 ura3 lys2 trp1 his3 leu2 DCP2::DCP2-yEGFP-kanMX4 BFR1:: natNT2-MET25-BFR1*	This study
YAS4048	Dcp2-GFP MET25-Scp160	*MAT a ade2::ARF1::ADE2 arf1::HIS3 arf2::HIS3 ura3 lys2 trp1 his3 leu2 DCP2::DCP2-yEGFP-kanMX4 SCP160:: natNT2-MET25-SCP160*	This study
YAS1188	YPH499 Dcp2-GFP	*MAT a ade2 ura3 lys2 trp1 his3 leu2 DCP2::DCP2-yEGFP-kanMX4*	This study
YAS3118	YPH499 Dcp2-GFP Δ*bfr1*	*MAT a ade2 ura3 lys2 trp1 his3 leu2 DCP2::DCP2-yEGFP-kanMX4 bfr1:: URA3*	This study
YAS1188	YPH499 Dcp2-GFP Δ*scp160*	*MAT a ade2 ura3 lys2 trp1 his3 leu2 DCP2::DCP2-yEGFP-kanMX4 scp160:: LEU2*	This study

Weidner et al. Fig S1

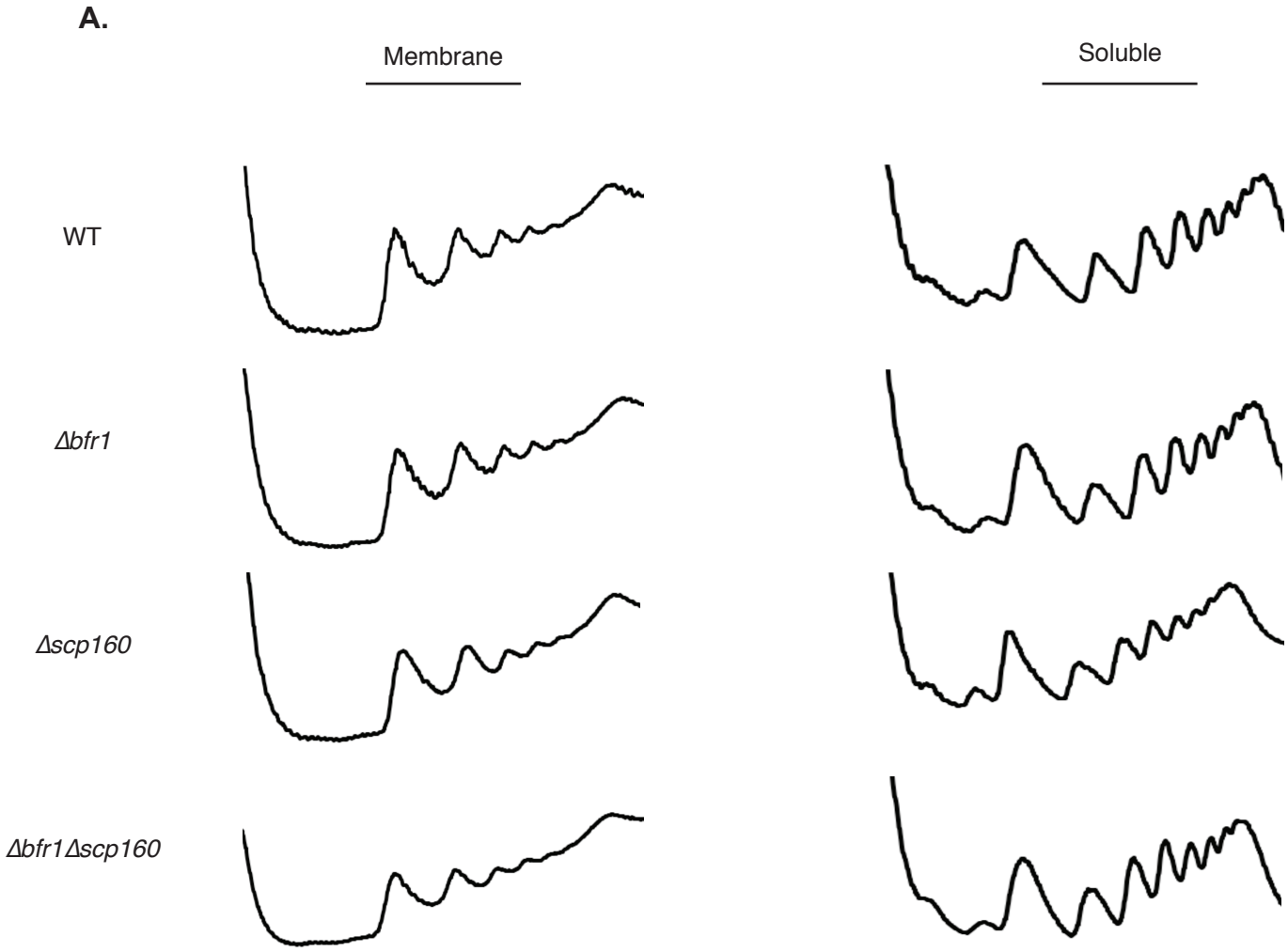

Weidner et al. Fig S2

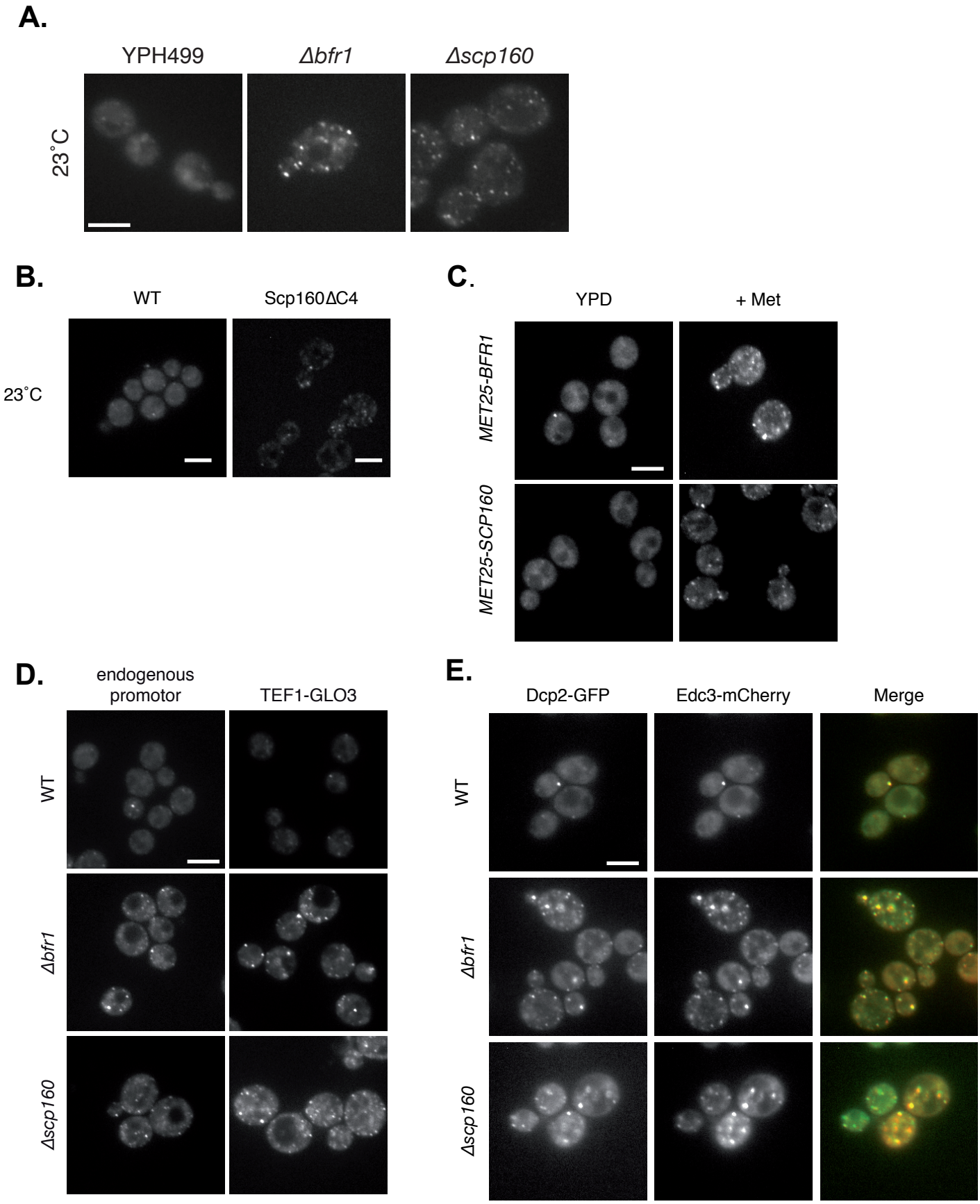

Weidner et al. Fig S3

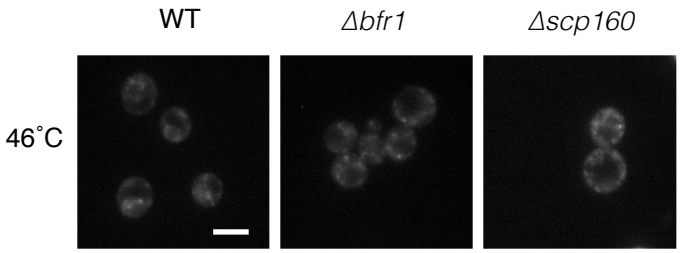

Weidner et al. Fig S4

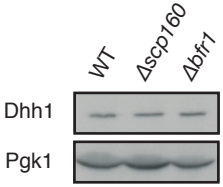

Figure S1. Polysome profiles from the membrane and soluble fractions remain unchanged in wild-type or mutant cells Wild type, Δ*bfr1*, Δ*scp160,* and Δ*bfr1*Δ*scp160* lysates were subjected to differential centrifugation at 13,000 x g to generate a membrane and a soluble polysomal fractions. The resulting fractions were then subjected to polysome profile analysis. In both the membrane fraction and the soluble fraction, similar polysome profiles were seen amongst the different strains. Due to less material being present in the membrane samples, the scale between the membrane and soluble fractions were adjusted to allow easier comparison.

Figure S2. (A) Deletion of *SCP160* or *BFR1* led to multiple Dcp2-positive foci. *SCP160* or *BFR1* were deleted in the wild type YPH499 in which Dcp2 was tagged with GFP. **(B)** Deletion of the last 4 KH domains in Scp160 results in multiple P bodies. The endogenous copy of *SCP160* was replaced through homologous recombination with the linearized plasmid pMS449, in which the 4 most C-terminally located KH domains of Scp160 had been deleted. This strain also contains Dcp2-GFP tagged. The cells were grown at 23˚C and P body formation was observed. Similarly to the Δ*scp160* strain, Scp160ΔC4 led to an increase in P bodies under normal growth conditions. **(C)** Loss of *BFR1* or *SCP160* through methionine shut-off results in an increase in P body number. Strains were made, in which the endogenous promoters of *BFR1* and *SCP160* were replaced by the inducible MET25 promoter to simulate deletion of the gene. After 72 hours of methionine treatment, the observed P body phenotypes in the shut-off were similar to the constant gene deletions. **(D)** Overexpression of an unrelated gene does not rescue Δ*bfr1* and Δ*scp160* phenotypes. Wild type, Δ*bfr1*, and Δ*scp160* cells expressing Dcp2-GFP and containing the ArfGAP Glo3 under the endogenous promoter or on a plasmid expressing *GLO3* form the strong TEF1 promoter were observed at 23˚C. In both Δ*bfr1* and Δ*scp160* strains, the increased level of *GLO3* mRNA did not affect the number of P bodies induced. **(E)** Different P body proteins co-localize in Δ*bfr1* and Δ*scp160* cells. Wild type, Δ*bfr1*, and Δ*scp160* cells expressing Dcp2-GFP and containing a plasmid expressing Edc3-mCherry were observed at 23˚C. In the majority of the cases Edc3-mCherry and Dcp2-GFP were seen to co-localize.

Figure S3. Heat stress induces P bodies in Δ*bfr1* and Δ*scp160* similarly to wild-type. Wild-type, Δ*bfr1*, and Δ*scp160* cells expressing Dcp2-GFP were shifted to 46˚C for 10 min before imaging. In all strains, P body formation was observed.

Figure S4. Dhh1 protein levels are similar in wild-type and mutant cells Whole cell lysates were prepared from wild-type, Δ*bfr1*, and Δ*scp160* cells expressing Dhh1-GFP. Lysates were separated by SDS-PAGE and Dhh1-GFP levels were assessed by immunoblot. In all strains, a similar level of Dhh1-GFP was observed. Pgk1 was used as loading control.